A Compact Machine-Learning Based Diagnostic Utility for Seizure Detection and Localization

by

Rebecca Jacquelyn Mackenzie

BS, Mathematical-Physics, State University of New York at Buffalo, 1989

MS, Bioengineering, University of Pittsburgh, 2001

Submitted to the Graduate Faculty of

The Swanson School of Engineering in partial fulfillment

of the requirements for the degree of

Doctor of Philosophy

University of Pittsburgh

2024

UNIVERSITY OF PITTSBURGH

SWANSON SCHOOL OF ENGINEERING

dissertation was presented

by

Rebecca Jacquelyn Mackenzie

It was defended on

March 19, 2024

and approved by

Dr. Jennifer L. Collinger, PhD, Associate Professor, Department of Bioengineering

Dr. Kacey G. Marra, PhD, Professor, Department of Bioengineering

Dr. Joseph C. Maroon, MD, Clinical Professor, Department of Neurosurgery

Dissertation Director: Dr. Aaron P. Batista, PhD, Professor, Department of Bioengineering

A Compact Machine-Learning Based Diagnostic Utility for Seizure Detection and Localization

Rebecca Jacquelyn Mackenzie, MS

University of Pittsburgh, 2024

Seizures are episodes of abnormally excessive or synchronous electrical activity of localized populations of neurons in the brain. Epilepsy is a condition in which these seizures are repetitive. Some half a million people do not respond to drug therapy, and surgical intervention is necessary. Multi-electrode EEG recording is an important diagnostic tool for pre-surgical planning in these cases. While EEGs have relatively good temporal resolution, they have poor spatial resolution. Therefore, the onset and localization of seizure activity can be difficult to determine by direct observation of the EEG record. If those EEG channels that show the earliest onset of seizure-like activity can be determined, then those channels, corresponding to locations on the cerebral cortex, can indicate sites for the surgical correction of epileptogenic foci. To assist the clinician in determining which channels correspond to the onset of seizure activity, machine-learning tool have shown promise. However, computer-based diagnostic systems that are portable and accurate are not readily available for use by clinicians, especially in underserved areas. Also, the numerous computer-based EEG analysis utilities that have been devised to detect seizures remain limited in one or more respects: 1. a lack of sufficient spatial resolution of the EEG signal to indicate activity at a specific electrode, 2. an inability to resolve both temporal and spatial information for the same EEG signal, 3. the lack of ability to store previous analysis sets, so the system can refine its learning accuracy using new data, and 4. the ability to be quickly and accurately run on a portable computer system for use in underserved, rural, or remote

geographical regions. Previously, I demonstrated that a relatively simple recurrent neural network was capable of seizure detection and localization from an EEG record. To improve on this system and address the four limitations listed above, I have developed a compact machine-learning utility based on my original system but with significant innovations. This system has shown its effectiveness in determining the onset and cortical localization of seizure activity from high-resolution EEG records.

Table of Contents

List of Figures

Preface

The research presented here has its origins in the work I did for an undergraduate senior project in 1988. At that time, my electrical engineering professor had discovered the existence of neural networks and wanted to apply them to a biped robotics project. Since he knew I had some small skill in wielding a soldering iron and in circuit building, I was recruited out of his Electrical Circuits II course to assist him in his endeavor. Within several months, I had learned enough about simple backpropagation neural networks to design a balancing system for a two-legged robot that I had also designed and built. It worked pretty well. At least the device, tethered to an IBM 386 computer, took half a dozen steps without toppling over. I later used the same neural network design as the basis for x-ray beam focusing system at Brookhaven National Laboratory's National Synchrotron Light Source. I left for Pittsburgh before I knew if they had actually used the system or had filed it away among their PDP-11 notebooks.

Soon after arriving in Pittsburgh and starting work on military AI systems at Carnegie Group, I enrolled as a non-degree student at the University of Pittsburgh and Carnegie Mellon University. Shortly after doing well in a couple of upper-level engineering courses, I made the bold decision to seek admittance to the University of Pittsburgh's new Bioengineering program. Considering my less-than-stellar and scattered undergraduate record, I am forever grateful and in debt to Professor Harvey Borovetz for giving me a chance to show what I could do academically – when not living a day-to-day existence on the streets of Buffalo, New York, and wondering if I was going to see the following day. Professor Borovetz did not know any of these background

details but purely out of kindness took a chance on me. I hope I have not given him too much cause to regret his decision!

Since then, I made it through Pitt's Bioengineering MS-thesis program, attended the University of Cambridge, worked as an EMT, serving the homeless and exploited of Pittsburgh, and maintained employment with a series of local engineering companies. During my early years in the Bioengineering program, Professor William Federspiel was the source of guidance and support, especially after I had taken a long break from my studies to adopt a daughter and begin a family with my husband, who had also graduated with an engineering degree from Pitt. During my MS program didactics, I had the opportunity to continue to my interests in neural networks. For a signals and systems course, I designed a neural network ECG diagnostic utility which worked well in classifying various arrythmias.

Continuing my work with neural networks during this time, I decided to apply for Pitt's Bioengineering PhD program. Again, with generosity and kind support, I started my next phase of education. Seeking an advisor for my PhD research, I had the immense good fortune to meet Professor Aaron Batista. My proposed research did not intersect much with his lab's work, but he found my initial presentation interesting enough to take me on as his PhD student. Since then, he has been both my mentor and, especially, a good friend. Along with the aforementioned faculty, I will count him as one of the high points of my protracted academic career. As I sought interested faculty to build my committee, I am privileged to have the kind support of Professor Kacey Marra, Professor Jennifer Collinger, and Dr. Joseph Maroon. They have been a source of expert advice and direction as I developed my research and produced this final report of the

results of that work. I also thank Dr. Arka Mallela for his advice on EEG recording techniques. Grateful thanks, too, to Professor Neeraj Gandhi for his continual support and encouragement. I am also thankful and continual amazed by the dedication and energetic work of the medical directors, advisors, and students of the Street Medicine at Pitt program that I co-founded.

None of the above would have ever been remotely possible without the unwavering support and patience of my family. To Linny, Paul, and Kelly – mere words of thanks are insufficient to express my gratitude for your years of support and relief that my academic journey has finally been completed.

It's been a long *long* and sometimes strange journey from the streets of Buffalo. That kid living day to day on those streets could have scarcely dreamt of the immense good fortune and many kindnesses the future held for her.

From my godmother and aunt on the Kahnawake Mohawk Reserve in Quebec:

Tekonnonwera:tons i:se ne akewatsihre tanon me aterohsera. Skennenko:wa.

"Be grateful for family and teachers. Great peace to all."

1.0 Introduction

1.1 Epilepsy

Epilepsy is a neurophysiological condition in which there is a synchronized disruption of the brain's normal electrical activity. The condition has been known since antiquity and a variety of natural and supernatural causes have been associated with it. It wasn't until 1924, when Hans Berger developed the technique of electroencephalography to accurately record the oscillations of neurons in the human brain, that epilepsy's true neurological origins could be studied (Panteliadis C, 2021).

It is now known that the abnormal, excessive, synchronous firing of coupled cortical neurons in localized groups is the origin of what is called a "seizure" (Jiruska P, de Curtis M, Jeffreys J et al. 2013). Seizures occur in well-defined regions of the cerebral cortex or hippocampus and propagate outward along neighboring neurons or along neuronal tracts. The propagation of the seizure signal is by the increasing synchronization of groups of oscillating neurons (Nunez P, Srinivasen R. 2006).

The term "epilepsy" itself refers to the central nervous system pathology in which there are a collection of seizures resulting from various causes. Epileptic seizures arising from a specific location in the brain is called a "focal epilepsy," and includes: frontal lobe, parietal lobe, occipital lobe, and temporal lobe epilepsies (TLE).

TLE seizures are the most common type of localized focal epilepsies, accounting for

about 60% of the patient population with focal epilepsies. TLE's can be caused by a variety of brain injuries or abnormalities, such as traumatic brain injuries (TBI's), infections, strokes, anatomical malformations, or congenital abnormalities (Oisorio, Zaveri, Frei, 2011). In adults with focal epilepsy, about 50% of them have had a previous brain injury and a common feature in temporal lobe seizures, stroke, and TBI's are abnormalities in the neurophysiological differential diagnoses (Bartolomei, Cosandier-Rimele, McGonigal, 2010). TLE seizure foci are localized in two regions of the brain: mesial TLE's localized in or close by the hippocampus, and lateral TLEs, localized in the outer layer of the temporal lobe. Meisal TLE's are the most common class of temporal lobe epilepsies and represent about 80% of that type (McIntosh W, Das J. 2022).

At a cellular level, recent single-cell analyses mRNA transcripts studies have pin-pointed large-scale changes in the cortical transcriptomes of principal and GABAergic interneurons as the sources of the epileptic pathology in humans. Pyramidal cells of the cortex are highly connected through these interneurons. It is also thought that the gap junctions between these pyramidal neurons permit low-resistance flow of current between adjoining cells. Thus, cells coupled across the electrical synapses become readily synchronized. Subsequently, the high-frequency action potentials and local synchronization of neurons occur, contributing to a spike event, as seen on the EEG recording. Recruitment of adjoining cells - and across longer tracts in the brain - propagate seizure event across the cortex (Pfisterer, Petukhov, Demharter, et al. 2020).

1.2 Population affected

Patients with epilepsy have always suffered from various discriminations, including employment restrictions, denial of health insurance, and even forced sterilization (Valeta, de Boer, 2010). Even though society evolved a more understanding and accommodating attitude to epileptics, persons with this affliction suffer time lost at school and jobs - and diminished chances at social interactions (Mlinar, Petek, Cotic, Ceplak, Zaletel, 2016).

Epilepsy is one of the most common neurological disorders and the incidence of new cases diagnosed through middle age is about 40 for every 100,000 members of the population per year in the United States. Children experience seizure disorders more frequently than adults and approximately 20% of these children do not respond to drug therapy, and subsequently require surgical intervention (Zack, Kobau 2017)

Epilepsy remains a global health issue, especially where there are significant disparities in health care. Such places are in rural, remote, and wherever medical care is not readily available to the population (Nicoletti, Giuliano, Colli, Cidero, Padilla, Vitte, Mayaregua, Martinez, Camargo, Zappia, Bartoloni, Gomez, 2018). In inner-city populations of the US, there are many people who have poor access to healthcare considered routine elsewhere. Access to proper healthcare for this population remains difficult due to the cost of medication, lack of adequate medical insurance, lack of easy access to clinics, and clinicians unwilling to serve them (Wen, Hudak, Hwang, 2007). Presently, one-third of U.S. adults go without the medical care they need, do not seek medical care when sick, or can’t obtain necessary medications for chronic conditions. Often, the choice faced by the underserved of the US population is whether

to buy food, pay the rent, or to pay for medical care (Kaiboriboon, Bakaki, Llatoo, Koroukian, 2013). In particular, patients with epilepsy in these underserved communities often have a variety of other critical medical issues, such as drug or alcohol addictions, mental issues, ADHD, physical injuries, which either obscure the origin of the seizures or exacerbate the condition itself (Seidenberg, Pulsipher, Hermann, 2009).

1.3 Treatment protocols, including surgical intervention

There is no known cure for epilepsy. After collecting a detailed medical history of the patient experiencing seizures, a regimen of drug therapy may be initiated to explore which drugs, at which doses, are effective in treating seizure episodes. About 70% of the US population affected by epilepsy eventually respond to drug therapy. The Epilepsy Foundation reports that medication fails to control epilepsy in about one-third of adults and approximately 20-25% of children. (Cascino G, Brinkmann B. 2021). The use of antiepileptic drugs (AEDs) requires a risk-benefit assessment for each patient to weigh the possible incidence of seizure aggravation, loss of effectiveness through tolerance, and unpredictability of side-effects (Schmidt D 2009).

In those cases where drug therapy has proven contraindicated or ineffective, surgical intervention is considered. The goal of this option is the complete resection or disconnection of the cortical tissue containing the seizure focus or foci. Usually this is reserved for patients who have 1. seizures originating from one part of the brain, and 2. the part of the brain involved is

not associated with a critical physiological function, such as speech, movement, memory, or vision (Culler G, Jobst B, 2022).

Precise diagnostic techniques are required to define the location and boundaries of the epileptogenic focus so that minimal tissue damage is caused by the intervention surgery (Rosenow F, Luders H, 2001). The EEG record is an essential component of this diagnostic step (Baumgartner C, Koren J, Britto-Arias M et al. 2019). EEG monitoring, sometimes performed in conjunction with MRI, is used in these cases to assist the surgeon in identifying the precise location of the seizure focus and assure a successful surgical outcome (Englot D, Nagarajan S, Imber B, et al. 2015).

1.4 EEG in the Diagnoses of Epilepsy

Namely: (1) what techniques for recording seizure activity exist? (2) which are useful in which cases, for example, would you use one outside of a clinic? (3) what do the signals look like? (4) how are these signals used to guide surgery?

If it can be determined which signals from the electrode in recording montage show the earliest onset of seizure-like activity in the EEG record, then these channels, corresponding to locations on the cerebral cortex, can indicate possible sites for the surgical correction of epileptogenic foci.

There are several main techniques of EEG data collection. Electrocorticography (ECoG),

or intracranial electroencephalography (iEEG) involves placing an electrode array directly on the brain's surface which has been exposed via a craniotomy (Connolly M, Sharbrough F, Wong, P, 2003). A less invasive method is scalp EEG recording and can be performed in an outpatient clinic. In some cases, particularly with chronic, intractable epilepsy, the patient may undergo longer-term EEG recording with an overnight or several days stay in a clinic or hospital. During this type of the procedure, the patient is also monitored with a video camera to record any physical activity associated with a seizure (Monif M, Seneviratne U. 2017).

Although iEEG can provide a more precise localization and time-onset of epileptic activity, it is costly, involving surgical intervention, and in-hospital stay. For patients in clinically underserved regions, access to this technique is often not practical or affordable. This is the case especially in rural areas and developing countries.

In cases where sophisticated EEG recording equipment and/or clinical expertise to interpret EEGs are not available, scalp EEG recordings are a useful tool for clinical diagnoses. It is relatively easy to accomplish, its cost is low, and the patient can be monitored over a long-period of time in their home or even in the field. However, there are a number of disadvantages with scalp recordings. With current technology, it can produce imprecise localization results due to a variety of recording effects from electrode placement, artifacts, and clinician misinterpretation. In long-term monitoring, visual observation of the massive amount of data obtained from scalp recording is not easily examined and interpreted with any degree of accuracy. In these case, brief episodes of seizure activity may be overlooked altogether (Liang W, Pei H, Cai Q, Wang Y, 2020).

Scalp EEG recordings have the lowest spatial resolution of a variety of physiological recording techniques – typically in the centimeter range (Figure). However, determining even the approximate location of a seizure focus can provide useful information for a clinician, especially in an emergent situation (Rodríguez Quintana J, Bueno S, Zuleta-Motta J, 2021).

An EEG recording, regardless of its type, requires an orderly array of electrodes, called a montage, to be placed on the patient's head. These montages correspond to specific locations on or in the cortex and are essential for seizure focus / foci localization. There are a variety of EEG recording montages, the most common of which is the internationally standardized 10-20 system. This system spatially divides the skull into increments of 10% or 20% arrangement of electrodes ensuring that each one is relatively positioned to all the others. This allows each EEG study to provide consistent results across a patient cohort, regardless of the different shapes and sizes of heads (Acharya J, Acharya V. 2019).

Larger montages can be used and those with 96 to 256 electrode arrays are not uncommon. However, choosing the optimal number of electrodes for a specific purpose is important to reduce the computational requirement, in time and cost, for extracting and analyzing the cortical signals of interest. A variety of channel selection algorithms have been developed for this purpose (Aloitaiby T, Samie F, Alshebeili S, Ahmad I. 2015).

In rural, remote, underserved geographical regions and for use by emergency medical services (EMS) in the field, the development of portable systems using a reduced electrode montage, optimized with efficient selection algorithms, for seizure detection and cortical localization is of considerable current interest – and the central focus of the research presented

here.

Regardless of the recording protocols or environment, the EEG record, of any length, can be difficult to interpret. Even expert neurologists can disagree in the analysis of a recording and are not able to correctly distinguish seizure, non-seizure, pre-seizure or artifact activity.

Studies have shown that EEG signals during epileptic seizures are non-Gaussian due to stochastic fluctuations in amplitude (Furui A, Onishi R, Akiyama T, et al. 2021). A variety of parametric and non-parametric time-frequency techniques are useful in delineating different EEG spectra classes according to frequency as well as the time onset of seizure activity. Independent Component Analysis (ICA) and Factor Analysis (etc) have been used to separate out independent frequency components in a complex EEG signal (Artoni F, Delorme A, Makeig S 2018).

Advances in more efficient electrode design and innovations in signal processing algorithms to interpret EEG signals continue to improve its utility (Casson 2019).

1.5 Current Limitations of EEG Analyses

Despite its proven value, EEG analyses still suffers from several important limitations. The EEG signal has a low signal / noise ratio since the seizure focus lies deep under bone and cerebral tissue. As noted, recording artifacts affect the reliability of detection and interpretation. Preprocessing the signal and the inclusion of various noise-reduction algorithms have helped address this limitation (Michel C, Brunel D. 2019). Additionally, the EEG signal is,

over large time samples, non-stationary and non-ergodic, resulting in the lack of reliable statistics to characterize the signal, especially across the physiological variations and types of pathologies present in a large patient cohorts (Loza C, Principe J, 2021). Fortunately, these limitations can be effectively ignored if the time sampling of the signal is kept small (~ 4 sec) – and there are sufficiently large samples of patient data with which to work (Bertram 2014). The variation of patient data is one of the main concerns addressed in the novel research described here.

Nonetheless, the downside of requiring large data sets has required the use of sophisticated algorithms to interpret the data. This is that they require the use of extensive computational resources – even up to the inclusion and purchase of super-computer time to process data. Obviously, such requirements are costly, time inefficient, and not at all amenable for use on portable computer systems, such as laptops. To overcome these particular challenges, new approaches in accurate and fast signal interpretation have been studied in recent years. Deep learning has provided several useful approaches in EEG feature extraction and classification for single patients and across patient cohorts. These innovations have become useful in handling the complex data sets of image and video – and the recent breakthrough in semantic analyses has produced impressive results in text interpretation and generation.

EEG has a high temporal resolution when compared with other techniques such as fMRI or PET analyses. Temporal precision in the millisecond range can be attained and the onset of seizure activity can typically be accurately noted. However, using current methods, the spatial resolution of EEG recordings, both scalp and ECoG, regardless of the type or number of

electrodes used, is typically restricted. However, recent advances in EEG analysis techniques, especially employing machine learning methods has increased the ability to localize the origin of seizure activity in the brain (Burle B, Spieser L, Roger C, et al, 2015).

Scalp electrodes cannot detect the electrical changes in a single neuron since the potentials are: 1. relatively very small in amplitude and 2. there is a distance between the electrode and cortical tissue, involving the layers of the cortex and cerebrospinal fluid. However, the pyramidal cells of the cortex have similar alignment such that the sum of the dipoles of the synchronized region yield an electrical signal that can be detected at the scalp surface (Beniczky S, Schomer D, 2020).

Interpretation of an EEG is also easily obscured by the presence of various artifacts, both physiological and non-physiological in origin. The former are interferences originating from the patient themselves: cardiac, respiratory, muscular, and overall movement of the body which can shift recording wires and the placement of electrodes. Non-physiological artifacts can occur from spurious electrical signals from nearby equipment (Kappel S, Looney D, Mandic D, Kidmose P. 2017).

1.6 Computer-Based EEG Analysis

To date, numerous computer-based EEG analysis utilities have been devised to detect seizure activity but all remain limited in one or more respects: 1. a lack of sufficient resolution of the EEG signal to indicate seizure activity at a specific electrode, 2. an inability to resolve

both temporal and spatial information for the same EEG signal, 3. the lack of ability to store previous analysis sets, either in the spatial or temporal domain, so the computer program is able to refine its learning accuracy as it tests new data (Askham A, 2023).

Nonetheless, computer analysis is a critically useful tool to analyze and characterize a variety of time-series characteristics of the EEG record that contain information about changes in the cortical state in various neurophysiological conditions. The use of automated methods in medicine are employable in an advisory capacity to detect clinically significant data and provide the clinician useful information with which to initiate appropriate interventions. The development of computer-based EEG analysis utilities now allows the automated examination of EEG records and has been of considerable utility in discerning details that might be overlooked or misinterpreted (Koren J, Herta J, Furbass F, 2018). The rapid improvement of computer technology, particularly in the increase of processor speed, the use of graphical processor acceleration, and decreased costs of memory greatly contribute to the ability for clinicians to collect and interpret EEG records. Also, the corresponding rise of new and efficient computer-based algorithms assists clinicians making difficult diagnoses. The field of artificial intelligence (AI) is one class of computer algorithms is now particularly useful in the clinical setting – and particularly useful in interpreting the results of EEG recordings in patients with a variety of neurophysiological conditions.

1.7 Artificial Intelligence [AI] for EEG Analysis

AI is a family of computer-based techniques to replicate human-like intelligence in decision making for a wide-variety of applications. There are many remarkable successes in the development of useful techniques that greatly surpass human-like decision making and pattern recognition in both speed and spatial resolution. However, A.I., regardless of the technique employed, is not a solution for all problems and, despite some current claims, the replication of human-level intelligence is far off (Zador A, Escola S, Richards B et al. 2022).

The many specialties of healthcare have seen a great increase of AI applications over the past decade to the point where the presence of computer-based diagnostics and treatment advisement is a topic of serious debate in the major medical journals. The potential for AI and Robotics to supplant the clinician has become the matter of debate – no matter how undesirable leaving a human out of the procedure of patient care might be. Nonetheless, AI has proven its worth in its ability to handle massive amounts of complex clinical data and provide useful conclusions for clinicians to consider when determining an appropriate course of treatment for a wide variety of medical conditions. The advantages of AI in reducing the time taken to reach diagnostic and treatment conclusions – along with accompanying economic savings – are now well proven and accepted in the medical community. In particular, recent tests with the temporal convolutional neural network architecture have proven effective in predicting patient length of in-hospital stay and mortality rates [Bednarski 2022].

Historically, AI is a relatively recent invention. However, the foundations for the current systems have their origins during World War II, when Alan Turing developed the basic ideas for

modern computing]Bernhardt 2017]. Within a decade, in 1956, Allen Newell, Cliff Shaw, and Herbert Simon, developed a program to imitate some of the problem-solving abilities of human (Gugerty, 2006). Their Logic Theorist is generally considered to be the first real AI. That year, it was presented at the Dartmouth Summer Research Project on Artificial Intelligence (DSRPAI), hosted by John McCarthy and Marvin Minsky, and the term "Artificial Intelligence" entered the mainstream of academic and industrial research (Russell S, Norvig P, 2020). From then, and until the early 1970's, with the improvement of computer speed and storage, AI began to gain popularity. A variety of AI algorithms have been developed over the years.

In particular, "neural networks," are inspired by basic neurophysiological principles - particularly "threshold logic" (continuous input to an all-or-nothing output) and Hebbian Learning ("cells that fire together, wire together"). In 1949, Donald Hebb published his The Organization of Behavior which presented his neurophysiological theory that persistent input to neurons leads to long-lasting synaptic organization (Hebb, 1949). This principle was summed up by Carla Shatz in a 1992 article for Scientific American as: "cells that fire together wire together" [Shatz, 1992]. In 1954, the first Hebbian network was successfully modeled on a computer at MIT. In 1958, a Cornell psychologist, Frank Rosenblatt, using the very simple linear input-output model based on the McCulloch-Pitts artificial neuron, developed the idea of the Perceptron (McCorduck P, 1979).

By the 1970s, computer systems and algorithms were beginning to be used regularly by clinicians for analyzing EEG data from patients (Gevins A, Yeager C, Diamond S, 1975). Since then, the sophistication and economics of computer-assisted analyses has increased to allow

almost any clinic to record, collect, and make diagnoses from EEG studies (Panteliadis, 2021).

Today, the use of computer-based utilities for seizure detection and analysis has an important place in clinics located in remote, rural, and underserved areas where access to sophisticated and costly diagnostic equipment is not readily available on-site. Even the use of telemetric advisement between an underserved area and a well-equipped metropolitan center can take time, especially in critical emergent cases, or be affected by poor transmission resolution – and, again, by subjective interpretation of the clinical expert at the other end of the transmission (Mani J, 2014).

Jean Gotman, of the Montreal Neurological Institute, was one of the first investigators to experiment with the use of an automated system to detect epileptic events in the human EEG. Several years after Prior and Ives, in 1976, he published his first paper on the subject (Gotman J, Gloor P. 1976). Later, in 1982, Gotman described a computer-based system designed to detect a variety of different seizures (Gotman J. 1982). Gotman also authored several studies with Ives, whose work was mentioned above (Gotman J, Ives J, Gloor P 1979).

More recently, in 1993, Qu and Gotman investigated the method of EEG feature-extraction as the basis of a nearest-neighbor classifier, a learning vector quantitization neural network. Their method employed EEG features extracted in both the time and frequency domains to detect the onset of epileptic seizures, including: 1) Average wave amplitude, 2) Average wave duration, 3) Coefficient of variation of wave duration, and 4) Dominant frequency. Subsequently, feature vectors from both seizure and non-seizure EEG epochs served as templates in the classifier. With this method, new EEG patterns were classified

according to the closest template vector in feature space. Qu and Gotman claimed a 100% detection rate with a false¬-alarm rate of 0.02 per hour using this technique on patient-specific EEG data. However, attempts to use this method as a general detection system were not successful (Qu H, Gotman J. 1993).

In 1996, W.R.S. Webber and his co-investigators used a standard multi¬layer-perceptron (MLP) neural network to investigate abnormal variations in the human EEG. The input feature vectors were classified into small seizure, large seizure, and normal groups. While the results of this system were encouraging, their system suffered from several restrictions, notably the use of a large number of statistical features, some of them correlated to a high degree, to represent the EEG (Webber W, Lesser R, Richardson R, Wilson K. 1996).

Other investigators have expanded on Qu and Gotman's work. In 1996, Weng and Khorasani used the feature extraction scheme proposed by Gotman in the development of an adaptive structure neural network, but the detection rate of this system was not very high (Weng W, Khorasani K. 1996). In contrast to Weng's technique, Pradhan, also in 1996, used the raw EEG as input to a neural network (Pradhan N, Sadasivan P, Arunodaya G. 1996).

In the early 90's, neural networks, a type of machine learning, were hailed as the solution for many intractable time-series problems. There were extravagant claims by numerous industries and data analysis service but most of these promises failed to produce the expected miraculous results. For a few years, a so-called "AI Winter," there was little progress in using neural networks as efficient problem solvers.

Then, in the early 1990's Yann LeCun and his team demonstrated a Convolutional Neural

Network (CNN) model, which aggregates simple features into progressively more complicated features, was successfully used in handwritten character recognition (LeCun, Y. Bottou L. Bengio Y., Haffner P. 1998).

The CNN algorithm includes two main stages: 1. computing of low-level features using convolution processing steps that encode spatial-temporal information and 2. input these low-level features into a classifier that captures high-level temporal information using a recurrent neural network. The main drawback of such an approach is that it requires the two separate processing steps. So, initially, CNN's remained a peripheral machine learning technique because researchers could not address the critical problem of scaling. Overcoming this problem necessitated large amounts of data and fast computer systems to be efficient. (Lindsay 2020).

Finally, in 2012, a new machine learning architecture, AlexNet, found that an increased number of processing layers in the model was needed for the useful resolution of complex images. At first, this architecture was computationally intensive, but the use of graphic processing units (GPU's), which could optimize computer memory utilization, greatly improved the speed of neural network training. This made it possible to use larger sets of training data that made more complex and efficient CNN's able to handle high-resolution computer vision problems – and could be applied to improving the resolution and efficiency of EEG analysis (Krizhevsky A, Sutskever I, Hinton G. 2001).

In 2016, Colin Lea proposed the Temporal Convolutional Neural Network (TCNN) - a refinement of the CNN – for video image partitioning, an important technique for computer vision processing. Whereas, CNN's required two steps of processing, the TCN architecture

provided a unified approach to process two levels of information hierarchically. Having an overall simpler architecture than combined convolutional plus recurrent processing stages, makes this a suitable choice for spatial and temporal processing of EEG data (Lea C, Flynn M, Vidal R, et al. 2017).

1.8 Clinical Significance of this Research

A number of computer-based systems have been developed experimentally for the identification of seizures but there remain several necessary improvements: 1. accurate resolution of seizure activity at a specific electrode; 2. resolution of both temporal and spatial information for each signal; and 3. the storage of previous analysis results so the system will improve its accuracy.

This research addresses the limitations described in the previous AI models. In particular, it is successfully demonstrated here that neurophysiological signals recorded from epilepsy patients can be analyzed by CNNs to precisely predict and localize seizure activity in the human cerebral cortex. Three objectives have been accomplished:

1. The design of a hybrid neural network architecture with improved spatial and temporal resolution that performs the detection and localization of seizures from scalp and intracranial EEG data obtained from epilepsy patients;

2: the retention of test results from each patient and each patient cohort that builds a database of new data to train and further test the utility;

3: the construction of a fast, robust, and fault-tolerant utility that is portable to a laptop computer and can be used by clinicians in remote, rural, and underserved areas.

Previously, I successfully demonstrated that a class of neural networks, recurrent neural networks (RNN's) which are useful for temporal pattern recognition, detected seizure-like activity as well as the localization of seizure foci in the EEG record of epileptic patients (Bates R. 2001). In this early work, EEG data that experts agreed contained seizure activity were collected as gold-standard records. These data have been retained as benchmark sets to obtain comparative performance metrics for the new systems developed here.

This earlier system was tested on subdural EEG data which increased the spatial resolution of seizure focus localization. In order to develop a system that is both portable, non-invasive, and easy to use, the new system was designed to use scalp data, using a montage with considerably fewer spatial placements of electrodes. To improve the spatial resolution of seizure focus localization with this method, a novel Volterra series based neural network is used, which considered the neighboring and next-neighboring electrode signals surrounding the central electrode. Progressing through the entire montage of the scalp recording provides a triangulated result of electrode signal strength. Using an algorithm similar to that used in GPS localization, an accurate position of the seizure focus is obtained (Craley J, Johnson E, Venkataraman A. 2019).

2.0 Methodology

Neural networks were considered for this particular study over other time-series techniques for several reasons. The main important feature of artificial neural networks is their ability to adapt to changes in their environment by modifying their connection weights. This property is especially useful for analyzing signal data in which there may be changes in the behavior of the signal at unpredicted times. Since the nodes of the neural network can be designed with nonlinear activation functions, nonlinear signals, such as EEG, can be analyzed – and since the network can contain a large interconnection of these nodes, fairly complex nonlinear signals can be analyzed. Previous work demonstrated that a relatively simple recurrent neural network architecture could accurately detect both the onset time and the cortical location of a temporal-lobe seizure from a patient's EEG record. In fact, the particular recurrent neural network designed and tested was capable of accurately pinpointing two separate epileptogenic foci in the EEG record from a pediatric epilepsy patient. This accuracy was confirmed by other more traditional methods and further validated when neurosurgery to excise the epileptogenic foci was performed, reducing the patient's seizure onset intervals from minutes to only a few per day, allowing the person to participate in more normal social and educational activities.

Some thirty years ago, designing a neural network was a much easier process than it is now. There were several categories of popular architectures that served a variety of purposes. Selecting and refining these architectures for a specific application was largely a matter of trial and error. This process was simplified by the availability of black-box functions which allowed for

fast prototyping of possible models, but left the inner workings and processes of the neural network obscured from the user. Since then, an explosion of innovations have made available a vast number of neural network architectures and refinements.

Building on my previous work, a temporal convolutional neural network (TCN) is specifically designed to run efficiently and relatively fast (compared with other neural network architectures, including Convolutional Neural Networks [CNN], as noted in the introduction section of this work) on a laptop computer, making it a useful diagnostic tool for use by clinicians in remote, rural, and underserved areas of the world.

To address the requirement for portability and detection accuracy, I employed several innovations in the design of the neural network presented here:

- The design of a temporal convolutional neural network
- The use of a Volterra kernel
- The use of the resilient backpropagation training algorithm.

A Volterra-Temporal Convolutional Neural Network [V-TCN] is designed and tested with high-resolution EEG data from two sources. The successfully tested data previously analyzed by the recurrent neural network [RNN] I designed is rerun as part of the validation set. Also, new data from the Temple University Hospital [TUH] EEG Repository is selected. The TUH EEG data is also high-resolution with 94 channels and seizure events for each data set have been annotated by experts. Both sets constitute the gold-standard test sets for this study.

2.1 TCN

The hierarchical structure of EEG electrode recordings containing components of seizure activity, pre-seizure activity, no-seizure components, and noise is particularly well handled by a TCN. Also a TCN contains a convolution step so that the influence of neighboring and next-neighboring electrodes are included for a more accurate resolution of the spatial component of the signal over time. Because of this ability, TCNs give excellent results compared to other detection algorithms for a number of pattern recognition tasks. This work has shown that very accurately trained TCNs are able to recognize specific patterns in EEG recordings and localize seizure events that may not easily discernible, even by trained and experienced clinicians. TCN's like CNNs employ convolutional layers, but adapt to temporally sequential data by using causal convolutions, in which the kernel only considers a current time point and point previous to that time point, thus preserving the temporal order of the EEG data. Furthermore, the essential property that makes TCN particularly useful for EEG analysis is that two-dimensional convolution kernel captures the spatial separation of each data point as well as their temporal distance. TCNs also are able to overcome "the curse of the data" since the windowed data is much smaller than the total input data. The initial TCN's tested for this project were designed to retain successful identification results so the utility improves its own accuracy in subsequent analyses of patient data. The accuracy of the final TCN designs is tested against the temporal-only results previously obtained and also against new patient data that contains gold-standard seizure activity data identified by a physician prior to a successful surgery. In addition to collecting new data, data from a previous set of patients, containing gold-standard annotations of seizure and non-seizure

events confirmed by epilepsy experts, is also included in this study to test the accuracy of the CNN system.

2.2 Volterra Kernel

The Volterra model is widely used for nonlinearity identification in practical applications and here we use it to calculate the nonlinear relationship between the EEG signal and its associated noise (Mitsis G, Marmarelis V. 2002). A Volterra series can be computationally intensive as well. As the ultimate goal of this work is to produce a utility that is fast and portable, a truncated Volterra series is calculated. Using the EEG signals from the central recording electrode, the immediately neighboring electrodes, and the next-neighboring electrodes, a third-order Volterra series approximation is used and found to be efficient for a pre-processing step.

A TCN using a Volterra kernel used in this study has three important advantages: 1) it is particularly useful for applications using small time-series samples that are causal and weakly nonlinear; 2) its use of polynomial activation functions, which may give the neural network a higher degree of resolution in pattern recognition; and 3) the ability to optimize its activation function to improve signal detection performance with regard to the EEG data from a particular patient, if the network is run in automated mode.

Since seizure events are not well-defined when observing data at discrete points in time, it is necessary to analyze the EEG records in the context of time correlated data segments. This requirement is met by designing the neural network to possess a short-term memory, so that

each data point is analyzed with respect to its neighboring point – and by designing the input layer to consist of nodes representing contiguous EEG channels.

The major limitation of using the Volterra kernel method is the number of coefficients required to model even a truncated series of a second or third-order series. To reduce the number of coefficients required to design a kernel that can be calculated quickly and still produce clinically accurate results, Laguerre orthogonal polynomials are used to estimate the kernels. The advantage of Laguerre polynomials is that they will converge quickly to the kernel roots. Therefore the computational time involved in calculating the convolution steps is much less than other usual methods. Also, since Laguerre polynomials are orthogonal functions, they tend to emphasize data near a training point – and deemphasize those points further way.

The complete mathematical development of the discrete Volterra kernel and Laguerre polynomial method I used in this work is included in the appendix of this document.

2.3 Resilient Backprop Training Algorithm

The resilient back propagation training algorithm is used for the TCN designed here. It has an essential advantage over the more commonly used backpropagation training algorithm: training with this algorithm is often faster than training with back propagation – an essential feature for a clinical diagnostic tool that needs to render useful information in a short time. In this algorithm only the signs of the partial derivatives of the function to be optimized and not their absolute values are calculated, thereby allowing for much faster training.

2.4 Design Assumptions

Time-series which are non-stationary poses additional problems for analysis by a neural network. A particular network which has provided reliable results for one section of data which is non-stationary, may produce spurious results for a subsequent section of data later in time. If the process generating the data is stationary and ergodic, there are a number of analytical methods which can be applied, but EEG data can be assumed to be neither ergodic or wide-sense stationary – unless the data epochs analyzed are sufficiently short.

Therefore, by making the assumption of slow time variation, one may divide the time-series sample into segments of appropriately small time-intervals (generally < 4 seconds) and assume each segment to be stationary in the interval – and, particularly, wide-sense stationary where its mean and its correlation function do not change in time. In addition, there are instances in which the variation of the EEG signal over even a small-time interval cannot be estimated by a sequence of stationary epochs without making some assumption about the smoothness of the time variation – *viz*. the second-order differences.

Neural networks are particularly susceptible to these first and second-order differences because of the inherent short-term memory which is a consequence of the network architecture. By making the assumption of the interval stationarity, it is assumed that these differences are small within each interval and that the transition between intervals is smooth.

Overfitting is especially dangerous because it can easily lead to predictions that are far beyond the range of the training data with many of the common types of neural networks. But underfitting can also produce wild predictions in multilayer networks, even with noise-free data.

The preferable strategy, then, is to design a neural network that is only as complex in terms of nodes and weights as it needs to be. With that in mind, the network architectures designed for this study were kept as simple as possible.

2.5 Additional Design Assumptions

As with the previous research, a number of important assumptions are made regarding the temporal and spatial characteristics of a EEG recording. These assumptions were used in the previous work and in this new design:

1. A seizure can be recorded as a time-series in two dimensions and are represented by 2D image with dimensions time of each data point x spatial ordering of electrodes [see figures 1 and 2 below]:

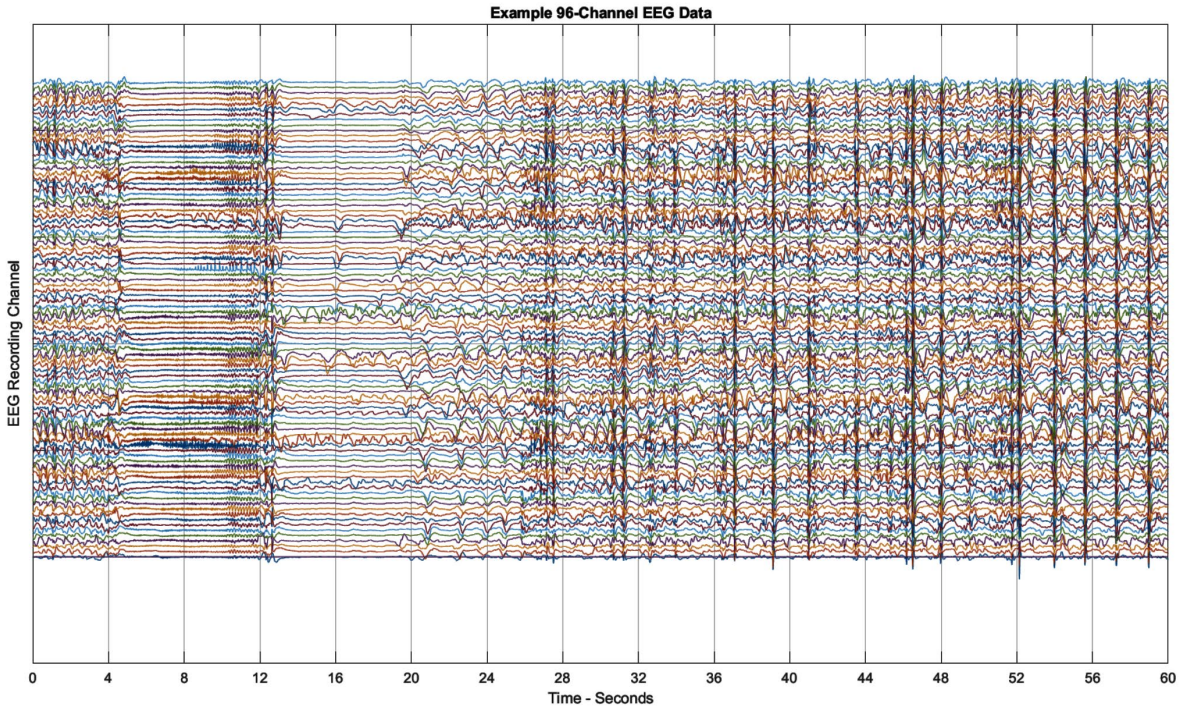

Figure 1. Example of an EEG sample of 96 channels recorded over 60 seconds.

2. A suitably small partition of a time series record [<= 4 secs] can be assumed to be ergodic and stationary.
3. The electrode recording is a sufficiently accurate measure of the EEG signal.
4. The resolution of the EEG recording is well approximated by the spacing of the electrodes, either on the scalp or subdurally.
5. The electrodes provide a useful approximation of the seizure focus / foci as well as the propagation of seizure activity across the cerebral cortex.
6. Seizure events may be linked by coupled oscillating neurons (several or many) synchronized over a larger area than represented by a single electrode.
7. Seizure activity can be linked over variable distances in the cerebral cortex (e.g. inter

hemispheric communication) disguising the original seizure focus.

Following assumption #1: the EEG montage is treated as a two-dimensional image, in which each "pixel" is an intensity of a discrete segment of the entire montage at some time, or, particularly, it is the value of each electrode at each time point of the recording. The input layer of the neural network consists of the image data along with two-dimensional spatial convolutions of each pixel with its nearest neighbors. Since we are localizing a focus (or multiple foci) of physiological activity over a two-dimensional space, viz. the cerebral cortex, a two-dimensional spatial convolution is appropriate.

This method calculates the two-dimensional spatial convolution of each electrode with its neighbors across the entire montage. In order to greatly reduce the computational requirements of these calculations only third order convolutions are calculated. As with the first method, each electrode is considered in turn as a central electrode along with its nearest neighbor electrodes and next-nearest neighbor electrodes.

Consider the following montage typically used in scalp electrode EEG recordings. This scheme is a good representation of the spatial configuration of the electrodes from which signals are recorded and analyzed in this study. As noted in the clinical significance section of this work, the most common epilepsies are temporal lobe focal seizures. Also noted is that about 80% of all temporal lobe seizures start in the mesial temporal lobe [MTLE]. All the data sets considered in this study are from MTLE patients and from the 94-electrode recording, signals 1 – 90 are analyzed, since the last 6 electrodes are records of signals from the EKG, limb, chin, and left and right ear and capnography recording electrodes.

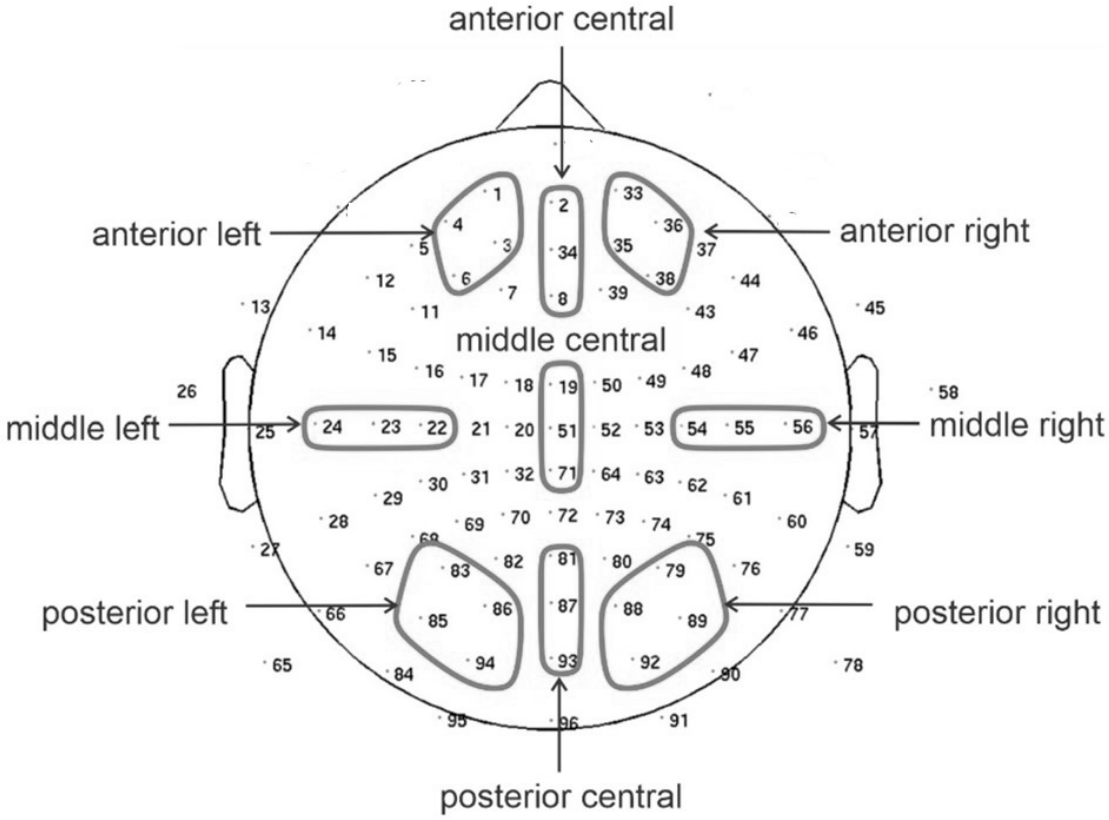

Figure 2: Example schematic of a typical electrode montage.

[from Nettinga, J., Naseem, S., Yakobi, O. et al. 2024]

The selection scheme for the EEG data is as follows: electrode date is taken from five signals – the central electrode and its four neighboring electrodes. The data for each set of five electrodes is test in 1000-point sets, corresponding to the 4 seconds required to maintain the condition of stationarity. When these first five sets are completely analyzed, the process is iterated one electrode – and one of the neighboring electrodes is now designated the central electrode. This iterative process continues until the entire 90 channels have been processed:

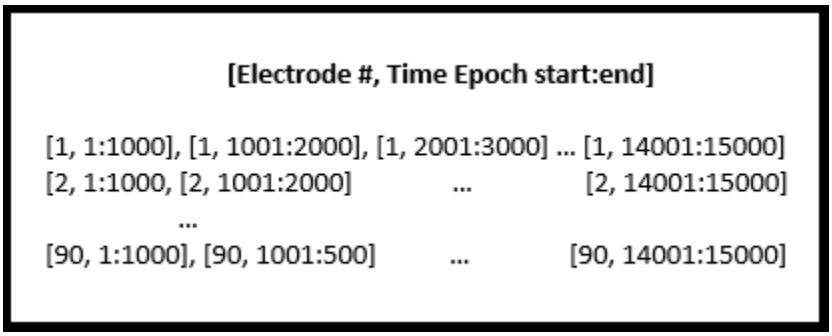

Figure 3. Construction of the temporal array of EEG partitions from the original sample.

The convolution kernel is then formed from the scaled amplitude values of these neighboring sets. Therefore, a second-order Volterra series is used in this analysis, which map the signal from a particular set of electrodes [n, n – M] to the output value y(n), where x(n) is the electrode signal amplitude averaged over the 4 second partition interval, equal to 1000 data points.

$$y(n) = \underbrace{k_0}_{central-electrode} + \underbrace{\sum_{m_1=0}^{2} k_1(m_1)x(n-m_1)}_{nearest-neighbor} \tag{2.1}$$

As a simple example, a second-order Volterra kernel calculation is depicted in the following figure. Here, a central electrode value is surrounded by eight neighboring electrode values. In actual practice, the numerical values in each cell would be floating-point numbers and rescaled on the closed interval [0.0, 1.0].

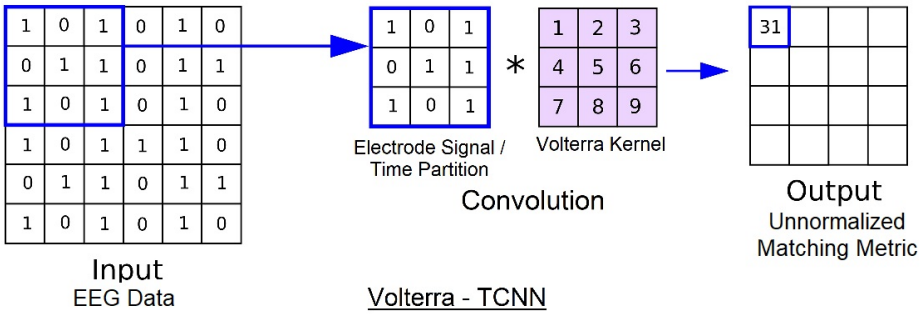

Figure 4. Example Volterra kernel calculation.

2.6 Data

Two sources of data are used in this study. The results from the previous work using the recurrent neural network are available and contain expert-verified seizure onset and localization results. These data are suitable for use in validating the structure and function of new architectures and are from a cohort of patients with idiopathic intractable temporal lobe epilepsy considered as candidates for neurosurgical intervention at the University of Pittsburgh Medical Center. As noted above, for evaluation of the new architecture, additional training and test data are obtained from the Temple University EEG Repository [TUH]. After the testing of the new data was completed, those results were compared with the results obtained from the previous study using the recurrent neural network. The TUH EEG data is in the EDF (European Data Format) format. The MATLAB *edfread* function is used to read the EEG data into tabular form readable by the TCN.

A total of 46 patient EEG data sets was obtained, all independent of each other ("subject-independence"). These sets were divided into 3 collections, each randomly collected: 26 for training, 10 for validation, and 10 for testing. Nine of the patient data sets were from adult males, 1 was from a pediatric patients. All were being treated for temporal-lobe epilepsy for which surgical intervention was indicated. No additional information was available – other than the expert confirmed seizure event localization annotations. Although the data was demeaned before being used, no other preprocessing was performed. Data sets of only 60 seconds duration met the study requirement that the system designed here is for use by non-experts treating various head trauma in underserved areas.

Each set contains 96 channels, 15000 EEG data points per channel, sampled at 250 points / second, yielding 60 seconds of data per channel. To meet the stationarity requirement, these 60 seconds of data were divided into fifteen 4-second partitions, giving 1350 4-second partitions per each 90-channel data set. For all twenty patient EEG data sets, this gives a total of 27000 4-second partitions to use as data for this study.

For training, these partitions were randomly collected to ensure independence between the samples.

The results of each test were retained and used for future training runs. Thus, as the most patients are tested, each with possibly unique seizure characteristics, the system builds up an "encyclopedia" of seizure events. These events are kept for each patients as well as each cohort of patients.

The overall data flow for this study is shown in the following diagram.

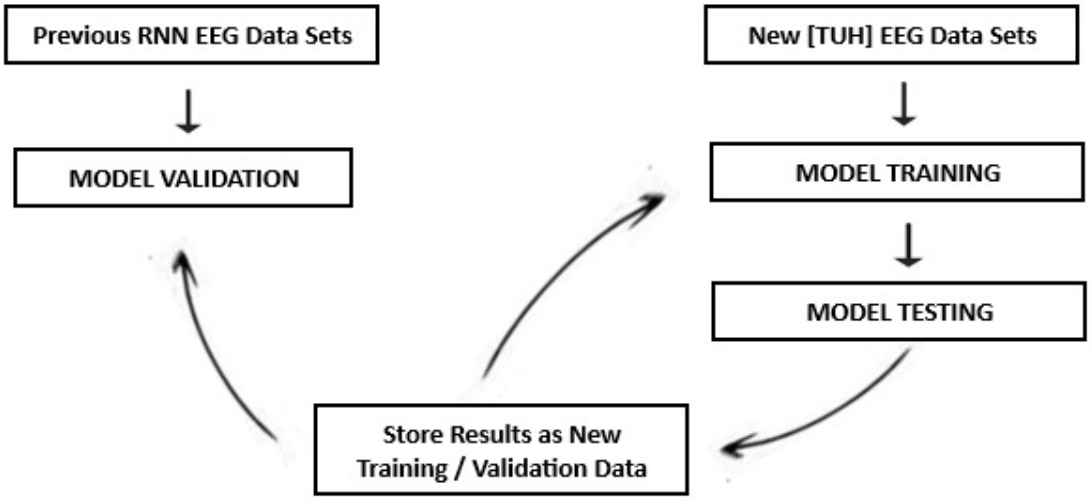

Figure 5. Data flow for the overall system.

The targets for these training sets are determined as follows: if the set of raw data corresponds to seizure data, its target is "1". If it corresponds to non-seizure data, its target is “0". Since the targets of this system were contained in only two classes – seizure and non-seizure, this allowed a more fast and efficient processing of the data. If the system were being required to distinguish between complicated images (e.g. tell a cat from a tea-cup), obviously far more data would be required.

The comparison between the outputs of the V-TCN and the expert annotated results were measured for each run of the patient test data. If the V-TCN detected a seizure within +/- 3 electrodes of the expert determined seizure event, then the analysis was considered to be accurate. This approximation is considered valid for several reasons, based on the results from studies undertaken by EEG experts:

1) the optimal spatial resolution of electrodes in various montage schemes (Feree T, Clay

M, Tucker D, 2001).

2) the optimal interelectrode spacing for scalp electrodes compared with epidural and subdural electrodes (Slutzky M, Jordan L, Krieg T, 2010)

3) the anatomical dimensions of typical seizure focus in the neocortex (Fauser S, Schulze-Bonhage A, 2004)

The overall method of using a V-TCN to analyze an EEG data set is described in the following steps:

Step 1. Consider the entire EEG record for a patient for a recording period [see figure 3]

eeg A

95x15000 double

	1	2	3	4	5	6	7	8	9	10
1	0.0700	0.0550	0.0300	0.0070	-0.0070	-0.0130	-0.0160	-0.0210	-0.0400	-0.0560
2	-0.3190	-0.3250	-0.3280	-0.3300	-0.3280	-0.3310	-0.3400	-0.3350	-0.3220	-0.3080
3	-0.2000	-0.1600	-0.1310	-0.1020	-0.0700	-0.0430	-0.0280	-0.0040	0.0280	0.0630
4	-0.1970	-0.1920	-0.1770	-0.1630	-0.1480	-0.1460	-0.1590	-0.1840	-0.1890	-0.1790
5	-0.3190	-0.3670	-0.4030	-0.4510	-0.4880	-0.5180	-0.5490	-0.5830	-0.6150	-0.6410
6	-0.4390	-0.4220	-0.4090	-0.4140	-0.4000	-0.3860	-0.3890	-0.3920	-0.4090	-0.4440
7	-0.3940	-0.4040	-0.4250	-0.4640	-0.5090	-0.5560	-0.6020	-0.6350	-0.6430	-0.6490
8	0.3470	0.3650	0.4090	0.4200	0.4220	0.4090	0.3980	0.3970	0.4000	0.4170
9	0.1420	0.1130	0.0750	0.0360	-0.0210	-0.0750	-0.1090	-0.1260	-0.1370	-0.1450
10	-0.8710	-0.8210	-0.7520	-0.6440	-0.5630	-0.4960	-0.4280	-0.3770	-0.3740	-0.4040
11	-0.0600	-0.0570	-0.0620	-0.0540	-0.0550	-0.0520	-0.0570	-0.0830	-0.1130	-0.1520
12	-0.3080	-0.3470	-0.3920	-0.4370	-0.4840	-0.5180	-0.5410	-0.5900	-0.6430	-0.6990
13	-0.5950	-0.6320	-0.6600	-0.6990	-0.7270	-0.7490	-0.7560	-0.7440	-0.7280	-0.7130
14	0.1040	0.1030	0.1100	0.1170	0.1190	0.1080	0.1000	0.0830	0.0750	0.0770
15	0.2790	0.2770	0.2760	0.2670	0.2580	0.2380	0.2080	0.1890	0.1900	0.1790
16	0.4160	0.4930	0.5610	0.6370	0.7150	0.7820	0.8280	0.8760	0.9220	0.9540
17	0.3350	0.4100	0.4670	0.5370	0.6110	0.6860	0.7340	0.7720	0.8120	0.8470
18	-0.3800	-0.2960	-0.2240	-0.1760	-0.1240	-0.0770	-0.0120	0.0450	0.1050	0.1500
19	-0.6360	-0.6590	-0.7010	-0.7390	-0.7720	-0.8190	-0.8550	-0.8890	-0.9230	-0.9800
20	-0.4630	-0.4770	-0.4990	-0.5040	-0.4960	-0.4900	-0.4770	-0.4700	-0.4750	-0.4710

Figure 6. A partition of raw EEG values from a larger data set.

Step 1. In the figure above The x axis corresponds to the channel number of the EEG recording montage. The y-axis is the time scale. In this particular sample, there are 4 channels (#1 – #20) over 1/25 second of data.

Step 2. Convolution: Using a window of some suitable dimensions [electrode]x[time] the dataset is partitioned into subsets by selecting one region of the dataset and then shifting over time.

Step 3. Each cell is then run through a "sorting" neural network and the network weights are maintained for all cells. Only those cells which show some or a lot of seizure activity are retained ("pooled"). Only those cells containing a threshold value decided on for seizure activity are kept. For example, if 0 represents a cell with no seizure activity and 1 represents the maximum seizure activity, it might be decided that any cell with a value over 0.8 is a cell with seizure activity.

Step 4. This much-reduced set of values then forms the input to a second neural network, which in this study is a recurrent architecture, which will determine which particular cell represents seizure activity in the EEG record. Those electrodes which show the highest seizure activity are then considered as sites for seizure origins.

As before, the values obtained from testing will be scaled over the continuous interval [0, +1] for ease of visualization in contour and graph plotting in which 0 indicate low seizure-like activity; +1 indicates a high-degree of seizure like activity. Values in between 0 and 1 will be compared against a set of patient-specific data which have been established as a gold standard by expert determination.

2.6.1 Output

The threshold value for the system is determined as follows: for the output range of values [0, 1], any value >= 0.90 is considered to be a seizure or seizure-like activity. (Previously, using a recurrent neural network for seizure detection and localization, I used a threshold value of 0.70). The TCN output is presented as a bar graph, with each bar representing the value at each electrode. For the examples below and in the results section, data sets with 95 electrodes are used to test the ability of the TCN to discriminate between closely placed electrode signals. The bar graph is a quick representation of seizure activity and readily noted by a clinician – one of the key requirements of this work.

In the following figure, threshold values of 0.85, 0.90, and 0.91 are shown. At threshold 0.90, there is a still a multiplicity of output values, so the threshold value was increased to 0.91 which allowed the system to choose a single dominant electrode, representing the most likely localization of seizure or seizure-like activity onset.

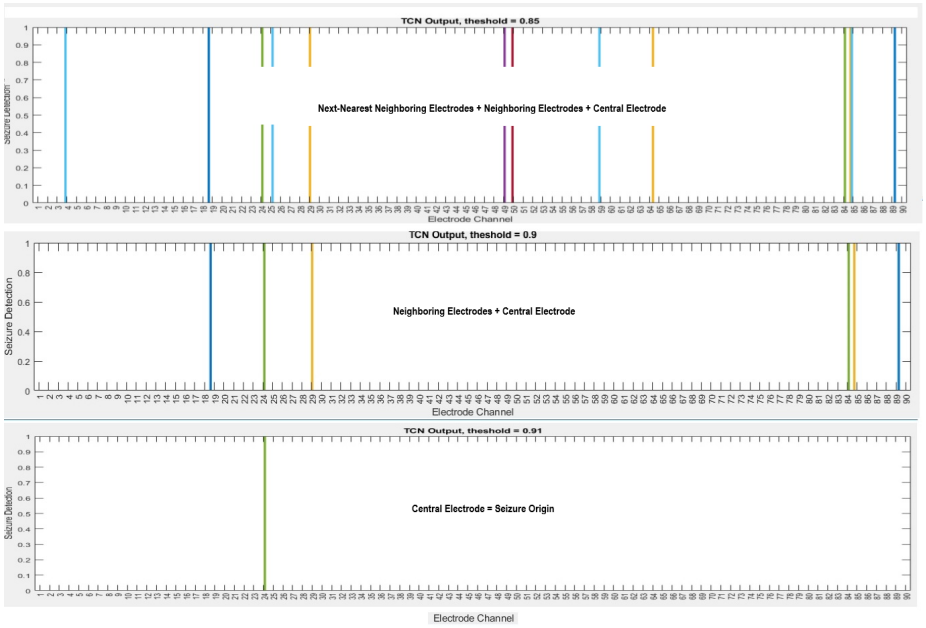

Figure 7. Detection of seizure-like events as a threshold for seizure/non-seizure is increased.

The lower thresholds might be the result of pre-seizure activity developing in the data set but this system is not trained to detect those events. Note that color of each bar does not indicate anything particular, but is merely used by the MATLAB Colormap to distinguish separate events.

The overall operation of the system is given in the following figure:

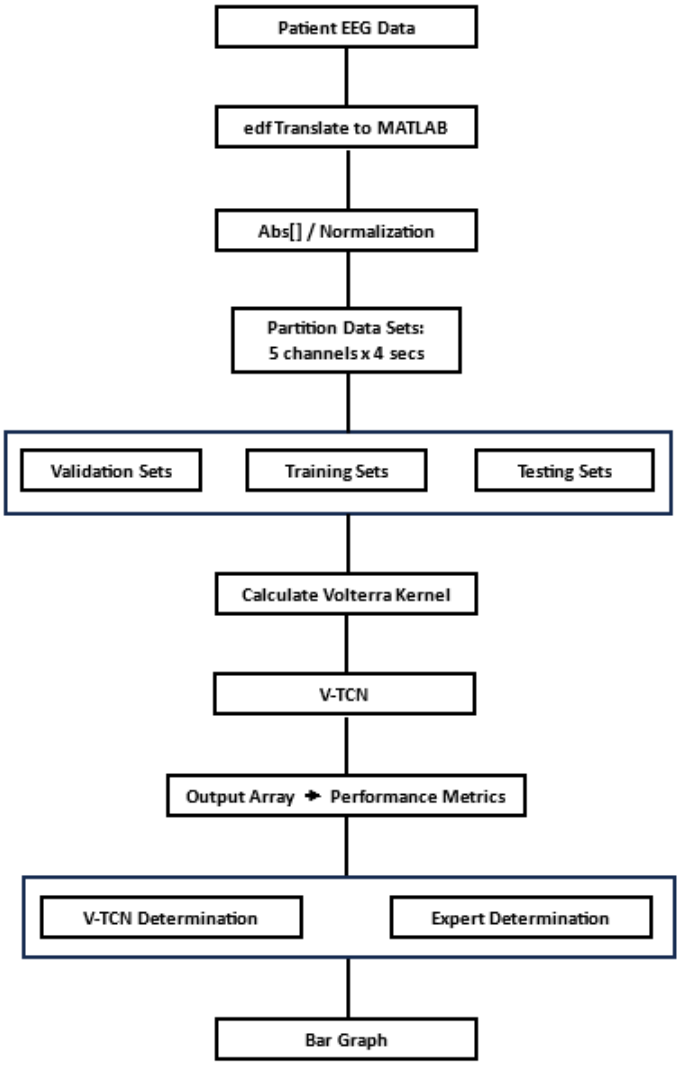

Figure 8. Overall schematic of the EEG data processing.

The following steps are illustrated in figure 11:

A) The patient data is obtained from an annotated, gold-standard, repository.

B) If the data is in EDF format, it is translated into MATLAB format.

C) The data is demeaned, normalized over the interval [0.0, 1.0]

D) In the scheme detailed above, 4 second samples of data each channel are selected.

E) These data are used to form three sets of input for the V-TCN: a validation set, a training set and a testing set.

F) For each sample, the second-order Volterra kernel is calculated using LYSIS in order to obtain the coefficients for the kernel.

G) The V-TCN is run for each sample and the output stored in arrays by MATLAB. As an option, the progression of weight optimization for the V-TCN can be calculated and examined to visualize how well the neural network is reaching the training goal.

H) Bar graphs are generated for the results.

I) (Not shown – post analyses metrics are collected to test the accuracy of the V-TCN to identify seizure activity.)

2.6.2 Performance Evaluations and Statistics

To test the efficiency of the final design in the field, the system was tested on four separate platforms: a Dell XPS 8940 11 generation Intel platform running Windows 11 22H2 and an Apple MacBookPro 18.1 Apple M1Pro running macOS 13.2.1.

To ensure accurate comparison of performance – as well as the portability of the code – the same utility was run on all four systems without any modification specific to the platform.

The final system design was trained, tested, and run under MATLAB R2023b.

As an initial test of the data, a periodogram of the test data is performed to confirm that a dominant seizure component exists.

To measure the performance of the final TCN design, four tests, usual metrics for

measuring the accuracy of a neural network model, are performed:

2.6.3 Best Validation Performance

The best validation performance metric calculates the training error for each epoch for the training, validation, and test performances. The object is for the training error to become less as more epochs of training are calculated. However, overfitting errors can cause this error to increase. This algorithm is designed to stop when the change in this error becomes small. Then the best performance metric is calculated from the epoch with the lowest validation error.

2.6.4 Confusion Matrix

The confusion matrix calculates the accuracy of the model. It charts the number of output values obtained from the predicted and actual values. The output “TN” stands for True Negative which shows the number of negative examples classified accurately. Similarly, “TP” stands for True Positive which indicates the number of positive examples classified accurately. The term “FP” shows False Positive value, i.e., the number of actual negative examples classified as positive; and “FN” means a False Negative value which is the number of actual positive examples classified as negative.

2.6.5 ROC (Receiver Operating Characteristics)

The ROC is a standard metric for data with two output classes, *viz* data that represents

either seizure or non-seizure events. This plot depicts the relationship between the true positive rate (TPR) for the model – model outputs that are above a pre-determined threshold value for seizure vs non-seizure and the false negative value – those values which do not meet the threshold value for a seizure event. The more accurate the model is in pedicting a seizure event, the closer the calculated ROC is to 1.0.

2.6.6 AUC (area under the ROC curve)

AUC provides a single-number metric to measure neural network performance. These values are calculted in the range [0, 1], with larger AUC values indicate better performance. A perfectly performing neural network will always correctly assigns positive class observations to the positive class, thereby generating a value of 1.0. The AUC is condiered to be better metric of neural network accuracy – the correct pediction of seizure vs non-seizure events against all the considered data.

2.7 Post-Testing Data

The results that met the metrics for seizure detection accuracy are stored and made avaialble for future trainnig and testing of the system, thereby providing a method for increasing the accuracy of seizure detection in future applications. The results are stored both as patient specific results, where the results for each parent are stored, and as a patient cohort database,

which store the results over a number of patients, thereby allowing the system to be tested for variation among separate patients (see following figure):

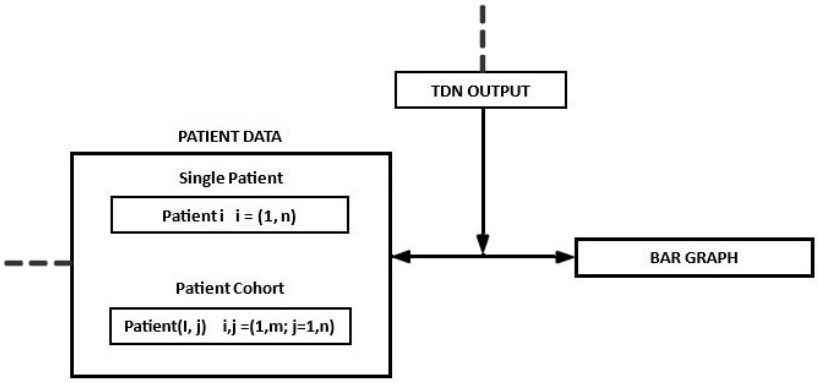

Figure 9. Collection of the output results and storage for future training of the system.

3.0 Results

Preliminary results from five patients are presented here. The Volterra-TCN system is first validated using gold-standard data. It is shown that the system met excellent performance metrics (see below). The system will be tested on a number of different portable platforms but the results presented for this initial set are from a PC. Also, to test the system's ability to discriminate between signals from electrodes close to each other on the recording montage, sets containing 95 recorded signals from a single patient are used here. A seizure detection threshold is determined as follows: on the closed interval [0.0,1.0], if the system detection is 0.90 or less, it is assumed that no seizure event was detected; a threshold equal or above 0.90 shows that a seizure event was detected at the electrode specified.

Although, there are a wide variety of techniques to present the seizure detection output of the system, a very basic bar graph is used here to make clinical application readily viewable. In the previous research, generating results from a recurrent neural network, a contour plot was used to plot the output from gold-standard data. Although these plots showed high-resolution depiction of seizure onset times and channel localization, visualization of isolated single channels was difficult (see following figure):

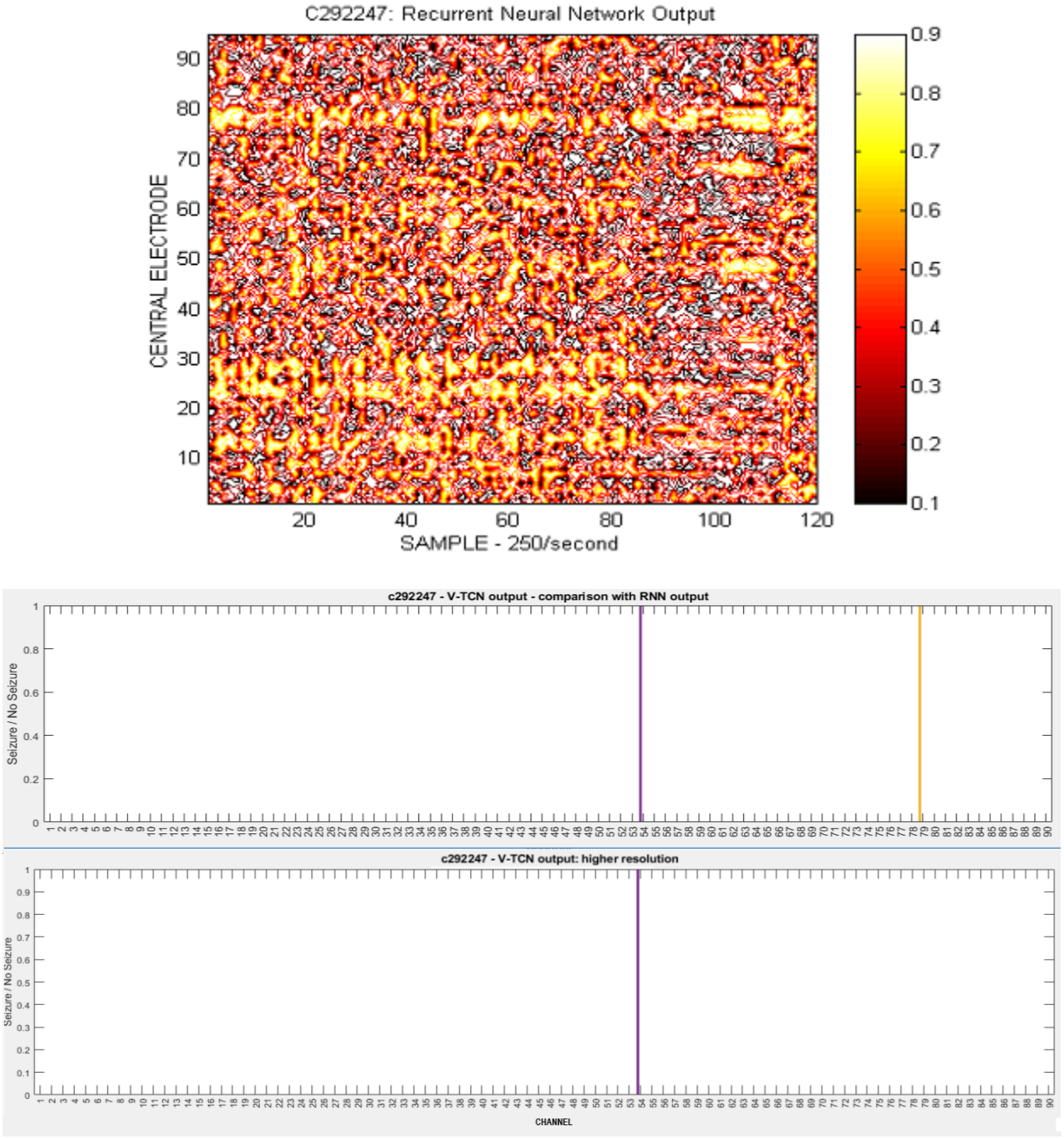

Figure 10. The system output shown as a MATLAB contour plot and a bar graph plot.

The current output scheme using the bar graph is included here as a comparison for clarity of results from the V-TCN. Also noted in the comparison of these plots is that the V-TCNN was able to produce a higher resolution than the RNN from the previous study, thereby eliminating signals which might have been erroneously classified as seizure activity. The V-TCN results presented above agree with the gold-standard data results.

In the five patient examples shown here, all sets detected seizure activity at a specific electrode, with the threshold at or above 0.9. One set did not reach 0.90, but was close at 0.89.

3.1 System Validation

1. Performance metric – comparison of three platforms
2. Validation – using known results from RNN
3. Training
4. Tests – 5 patients

3.1.1 Patient EEG Validation, example set

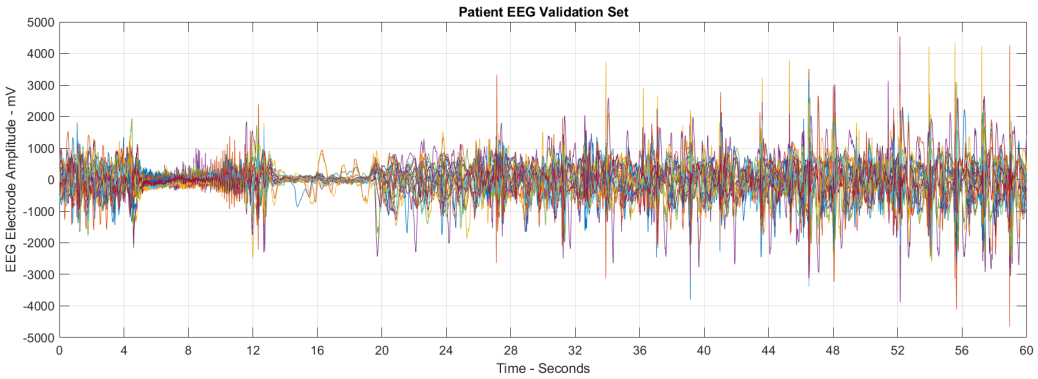

Figure 11. Sample of the EEG data set used for system valididation

In the above figure, refer to figure 2 for an expanded view of this set.

This example shows an apparent onset of seizure activity between 4 and 20 seconds.

The neural network located the precise electrode and time onset at channel 24, which is confirmed by expert gold standard.

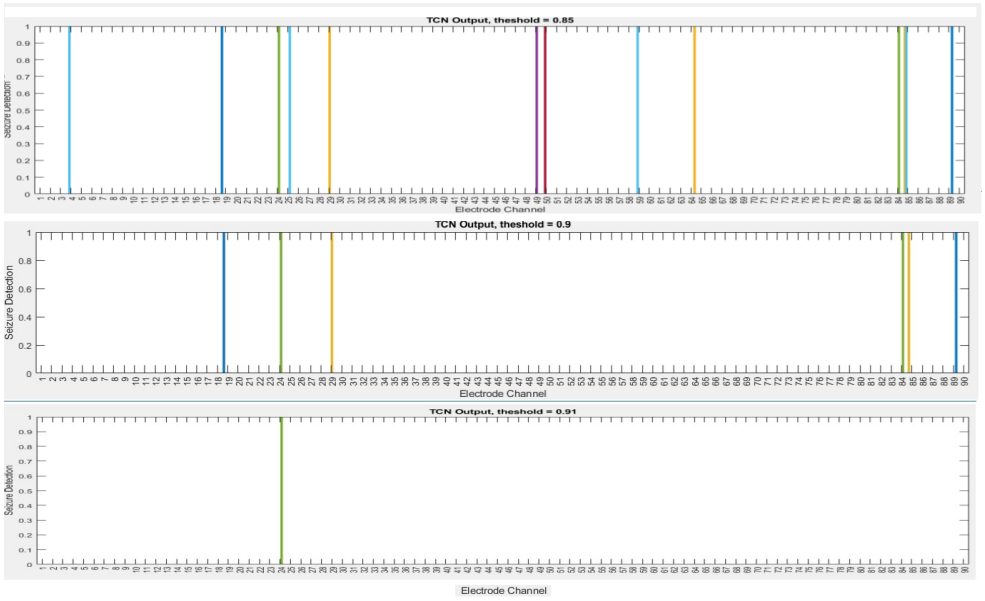

Figure 12. Output of the system at various thresholds. As the threshold level increases, possible non-seizure events are discarded leaving the only output the reach or exceed the 0.90 threshold.

The PC shows are very short training time. Even the cache is cleared before each test run, the system maintains an ongoing library of previous tests that met the =>0.90 threshold requirement for seizure detection. These data are then automatically added to any new training set to increase the accuracy and speed of training for any new tests. Since the TCN weights are already optimized from previous tests, any new tests should show improved training times and accuracy, as shown here:

Training Results

Training finished: Met validation criterion

Training Progress

Unit	Initial Value	Stopped Value	Target Value
Epoch	0	15	1000
Elapsed Time	-	00:00:04	-
Performance	0.353	0.0405	0
Gradient	0.341	0.0106	1e-05
Validation Checks	0	6	6

Figure 13. The results of a training run showing the number of epochs required to reach the specified target value.

And the validation performance plot is presented here:

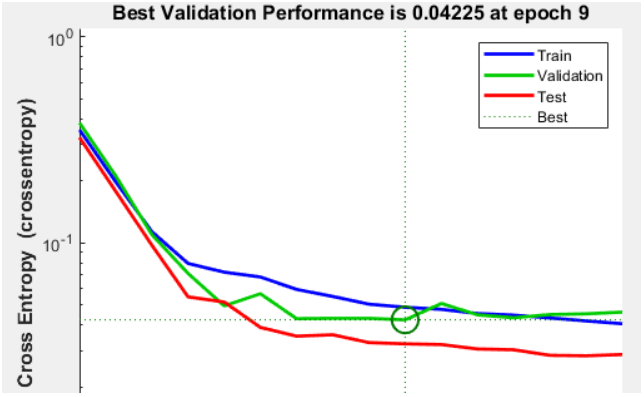

Figure 14. The validation performance plot

As noted in the methodology section, additional training epochs should reduce the training error except in the case of overfitting of the training data. By default the training stops here after six consecutive increases in validation error. In the above graph, this occurs at the ninth epoch of training.

3.2 Training

One of main tools used to evaluate the performance of the V-TCN before testing actual patient data is the calculation and plotting of a confusion matrix. This tabulation of validation results summarizes the performance of the V-TCN ability to correctly classify results.

The best resolution the V-TCN could make is partitions of 4 seconds. Each set of 15000 data points per channel, sampled at 250/sec, yielded 60 seconds of data and 15 4-second partitions. For 30 samples of EEG tested for validation – 90 channels per sample - this yields 2700 possible correct channels on which a seizure event was located for the complete set of all 30 tests. Since only one seizure focus was noted for each of the 30 samples, the total number of correct detections of seizure activity cannot exceed 30. The one exception was the EEG sample with the bilateral tonic-clonic seizure sample that showed two possible foci. However, it is not known which focus initiated the seizure activity – and if the two foci are entrained. In this case, the sample is considered to have a single correct channel localization.

Noted previously, 13500 partition samples of 4 second intervals, derived from the gold standard data sets, were used in the validation step. The results from the V-TCN confusion matrix calculation, counting the number of times a seizure was located or not located:

- True Positive (TP) = 8843: the model accurately predicted a seizure event 65.5% of the time.
- True Negative (TN) = 3526: the model accurately predicated no seizure event 27% of the time.

- False Positive (FP) = 580: Type I Error: the model incorrectly predicted no seizure activity as seizure activity 4.3% of the time.
- False Negative (FN)= 526: Type II Error: the model missed predicted seizure events and classified them as no seizure 3.9% of the time.

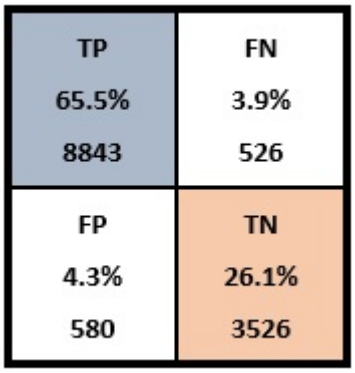

Figure 15. Confusion matrix for the V-TCN validation data

The confusion matrix shown in figure 18 shows the distribution of true positives, false positives, true negatives, and false negatives.

Using the results calculated in the confusion matrix, the accuracy of the model to identify true seizure events and discard those events which do not contain seizure events can be calculated:

3.2.1 Accuracy, ACC

$$ACC = (TP + TN)/(TP + TN + FP + FN) = 0.917 \quad (3.1)$$

From these validation metrics – and accounting for acceptable round-off error in the validation calculations, 0.90 is used as the threshold value for the V-TCN for detecting seizure activity in the data.

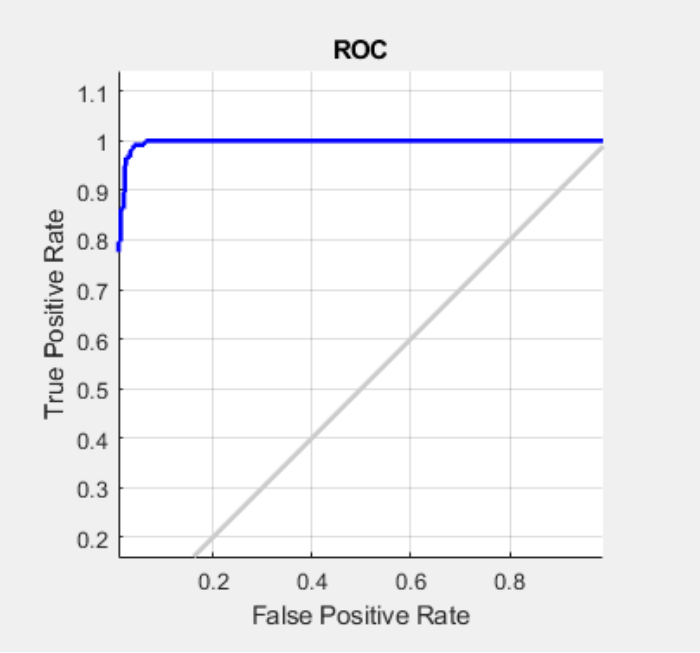

Figure 16. The receiver operator characteristic (ROC) curves

The ROC shown in figure 19 summarize the true positive and false positive predictions. The closer and faster the curve maximizes to 1.0, the better the ability of the system to discriminate between actual seizure events and false seizure events

3.3 Patient Tests

Ten patients, presenting with temporal lobe epilepsy, are selected to demonstrate the preliminary results for the application. Results 1 – 9 are from adult males; number 10 is from a pediatric male patients. All have been diagnosed with intractable epilepsy. Note that the plot trace and bar colors suggest no particular significance but are merely the random choice of the MATLAB colormap.

3.3.1 Patient 1

For this set of patient tests, the progression of threshold discrimination is shown to demonstrate how the system advances through the system by using 1st-order, 2nd-order, and, finally, the 3rd-order Volterra kernel to calculate the detection of a seizure event. In this example, the system locates the initial seizure event on electrode #59, which corresponds to the gold-standard annotation

In the other tests presented here, only the final, 2nd-order, threshold calculation is presented.

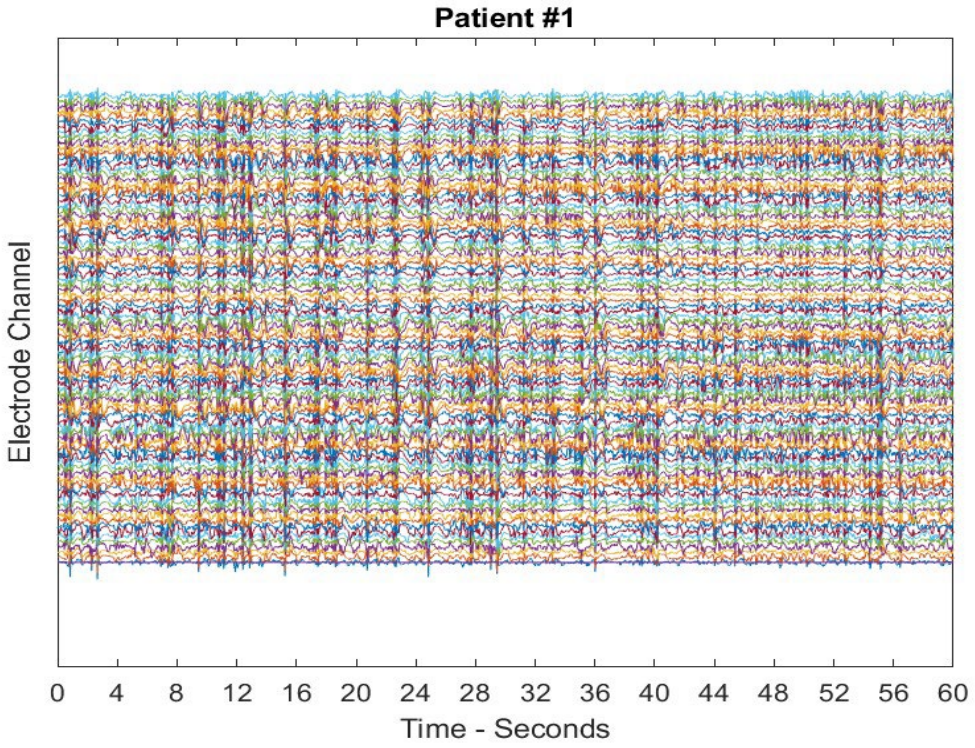

Figure 17. Patient #1.

Figure 17. (continued)

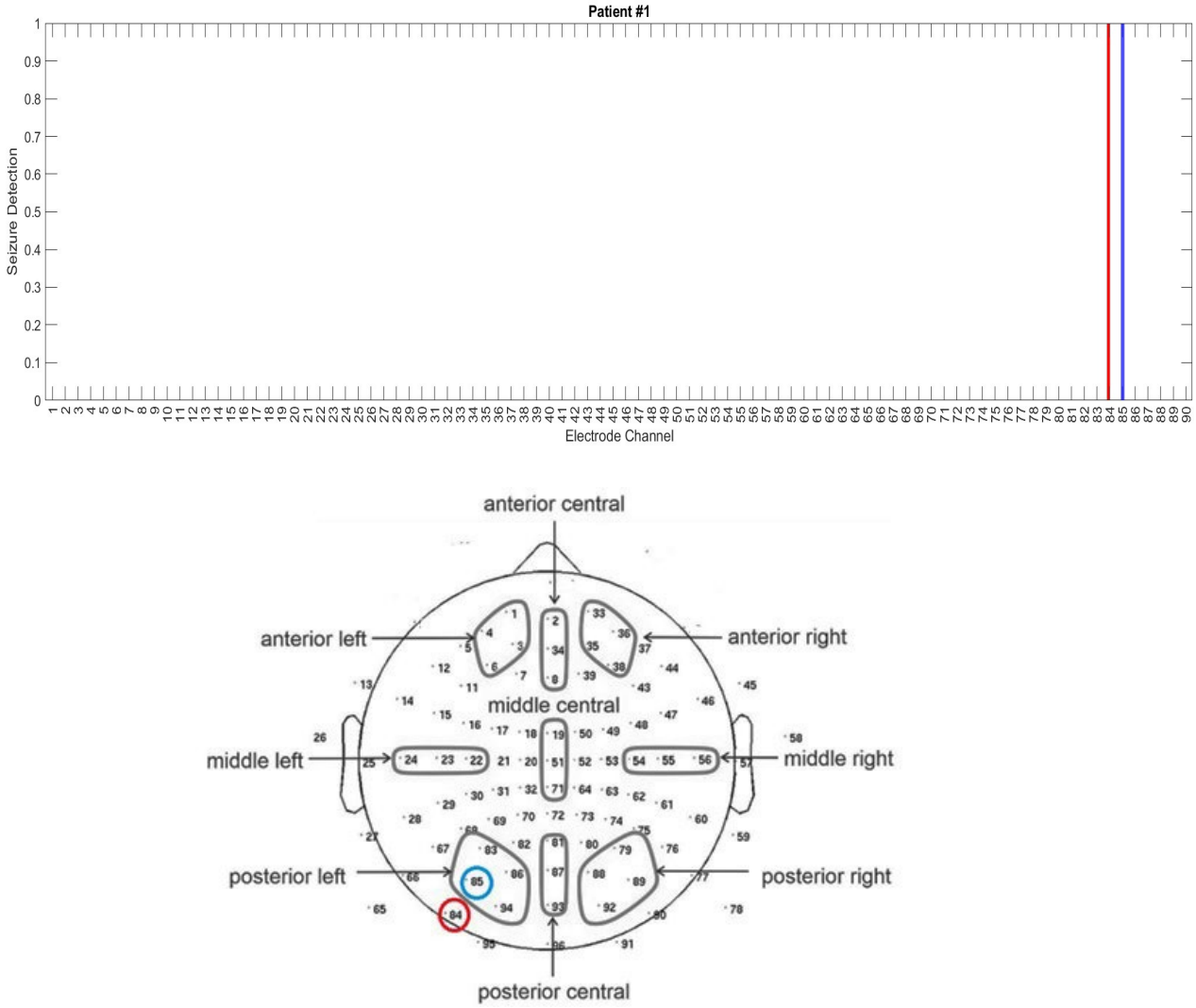

The results from patient #1 are as follows: a. The top figure is the original EEG record obtained from the patient. b. The V-TCN identified of a seizure event in the EEG record of an adult male with intractable temporal-lobe epilepsy. The expert-annotated result (shown in blue) is within two electrodes of the result obtained by the system. c. The location of the seizure foci on the EEG montage. The red circle indicates the focus location determined by the V-TCN; the red circle is the expert determination of the focus.

3.3.2 Patient 2

Seizure detection at electrode 85.

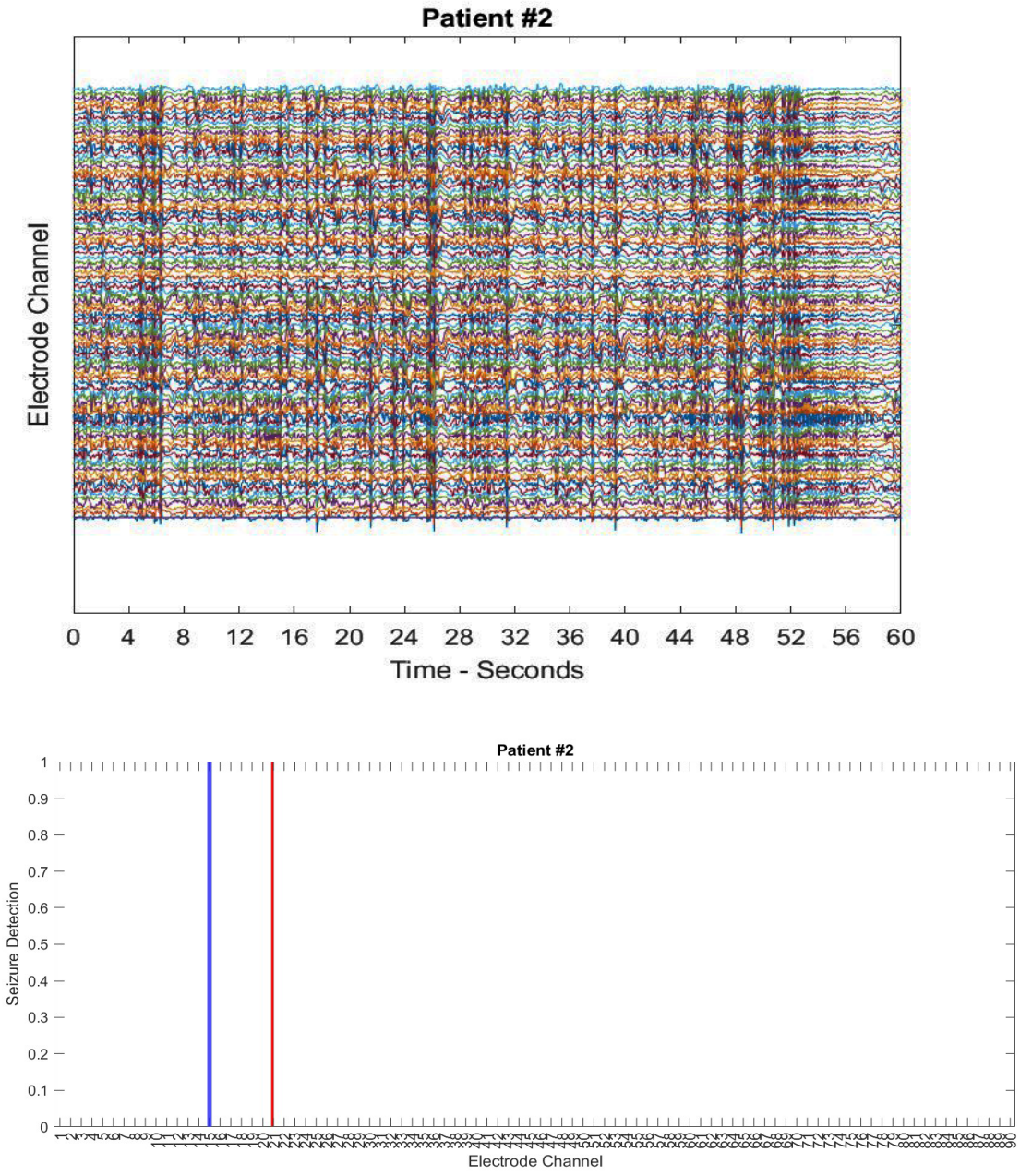

Figure 18. Patient #2

Figure 18. (continued)

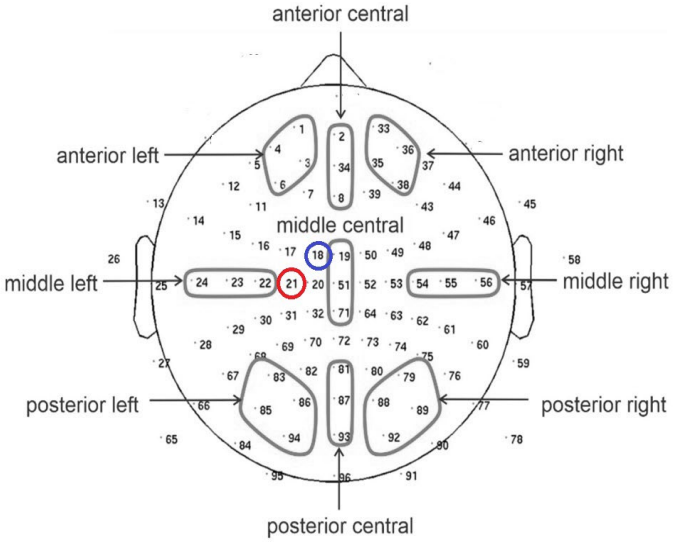

For patient #2: a. The top figure is the original EEG record obtained from the patient. b. The V-TCN identified of a seizure event in the EEG record of an adult male with intractable temporal-lobe epilepsy. The expert-annotated result (shown in blue) is within two electrodes of the result obtained by the system. c. The location of the seizure foci on the EEG montage. The red circle indicates the focus location determined by the V-TCN; the red circle is the expert determination of the focus.

3.3.3 Patient 3

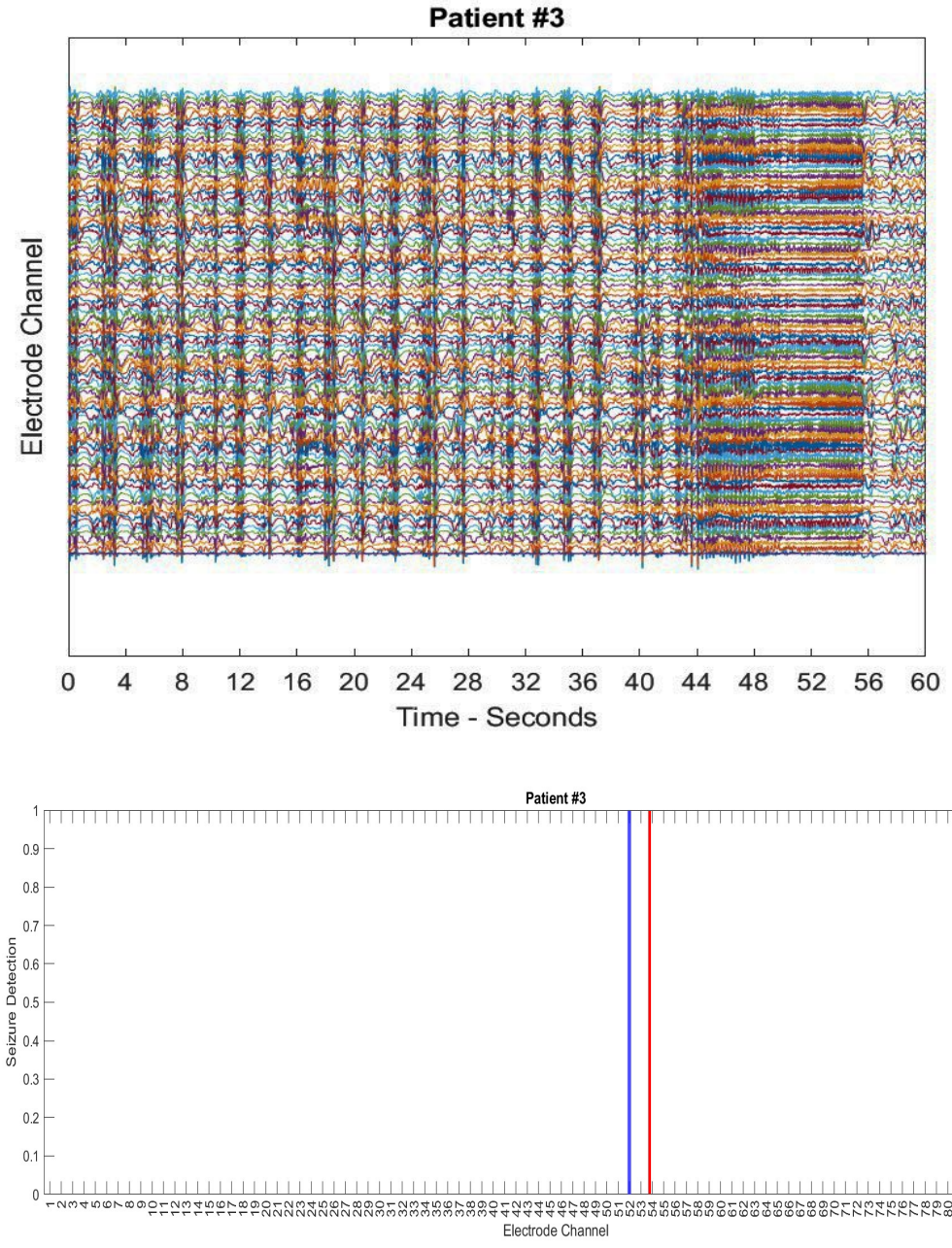

Figure 19. Patient #3

Figure 19. (continued)

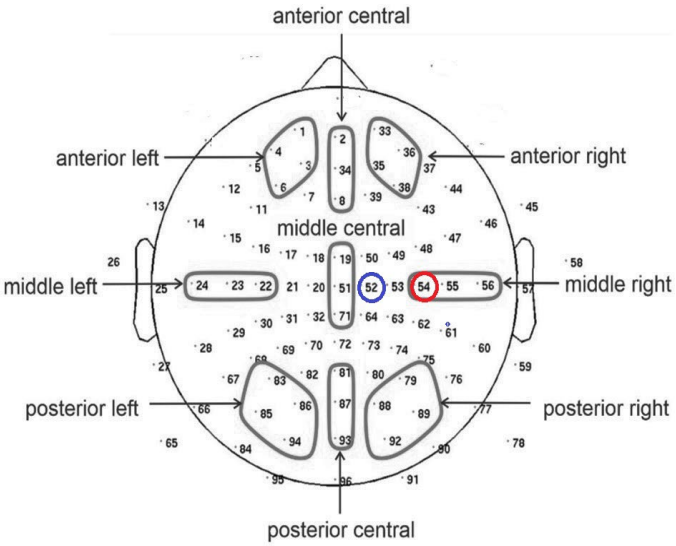

For patient #3: a. The top figure is the original EEG record obtained from the patient. b. The V-TCN identified of a seizure event in the EEG record of an adult male with intractable temporal-lobe epilepsy. The expert-annotated result (shown in blue) is within two electrodes of the result obtained by the system. c. The location of the seizure foci on the EEG montage. The red circle indicates the focus location determined by the V-TCN; the blue circle is the expert determination of the focus

3.3.4 Patient 4

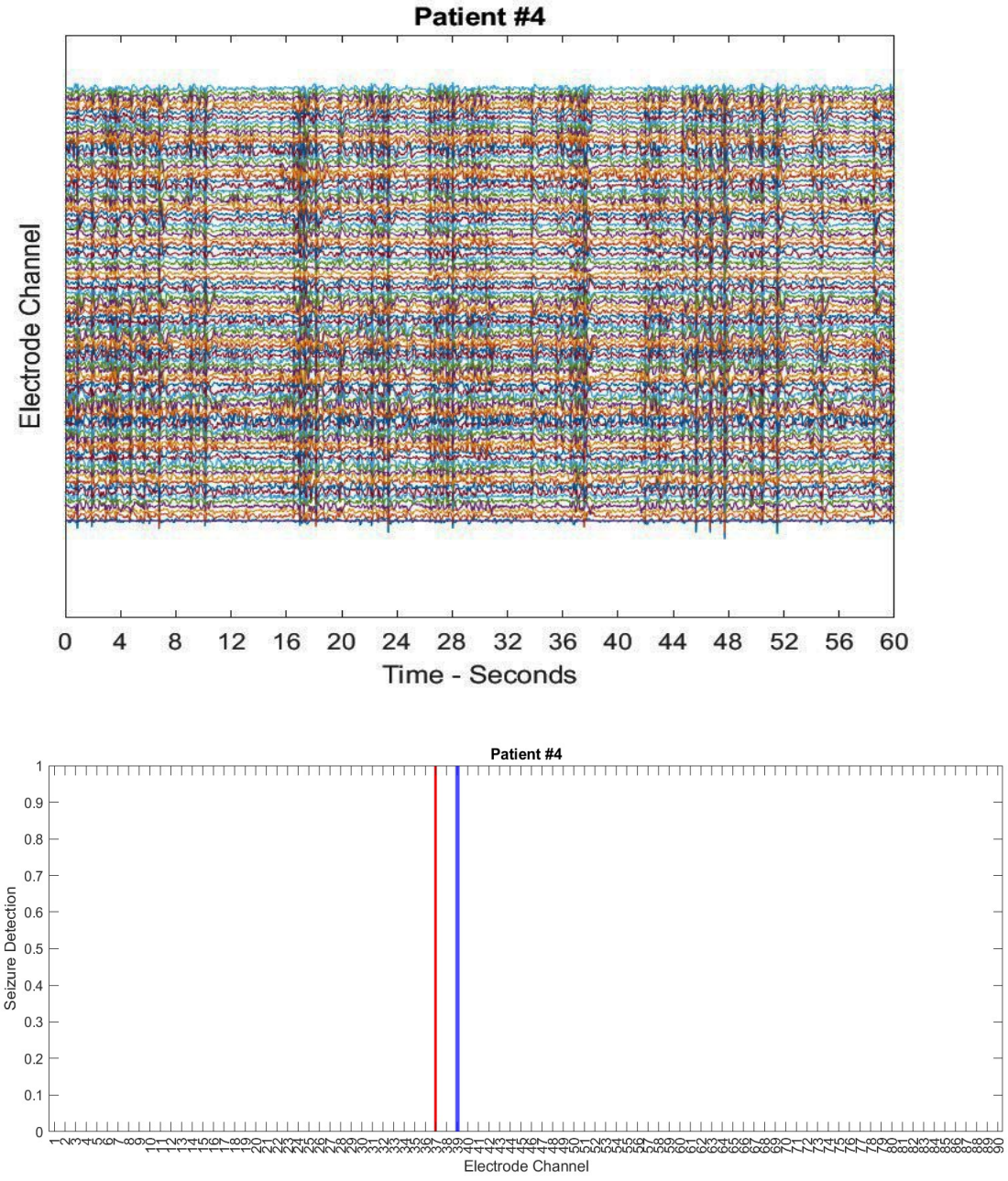

Figure 19. Patient #4

Figure 20. (continued)

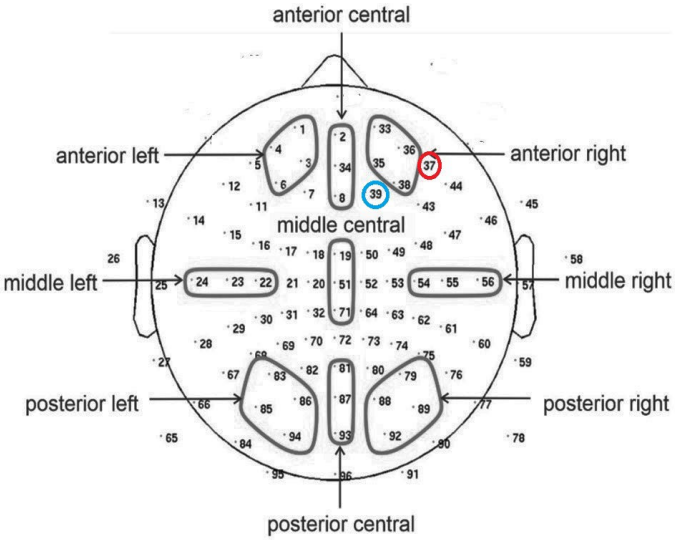

For patient #4: a. The top figure is the original EEG record obtained from the patient. b. The V-TCN identified of a seizure event in the EEG record of an adult male with intractable temporal-lobe epilepsy. The expert-annotated result (shown in blue) is within two electrodes of the result obtained by the system. c. The location of the seizure foci on the EEG montage. The red circle indicates the focus location determined by the V-TCN; the blue circle is the expert determination of the focus

3.3.5 Patient 5

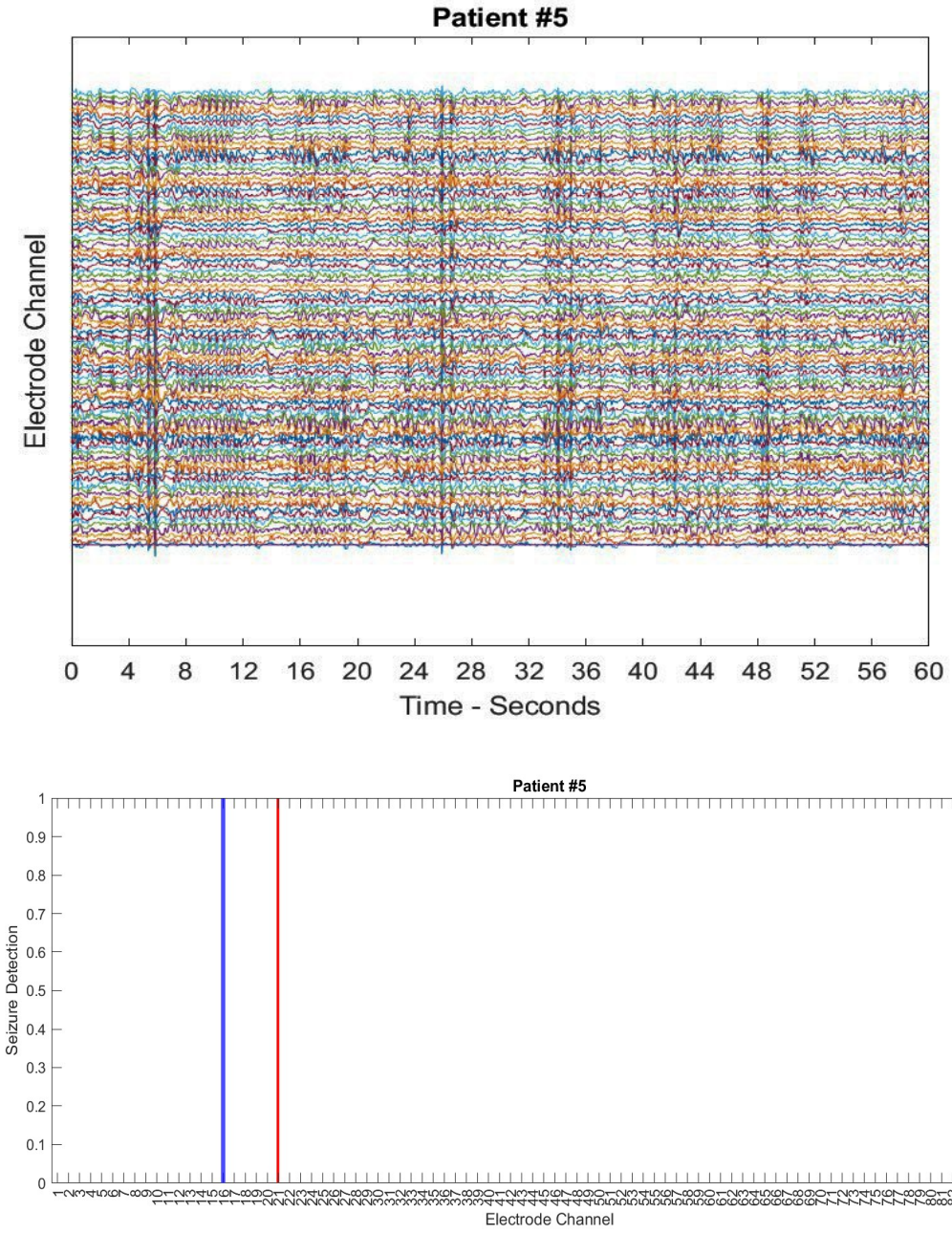

Figure 20. Patient #5

Patient 21. (continued)

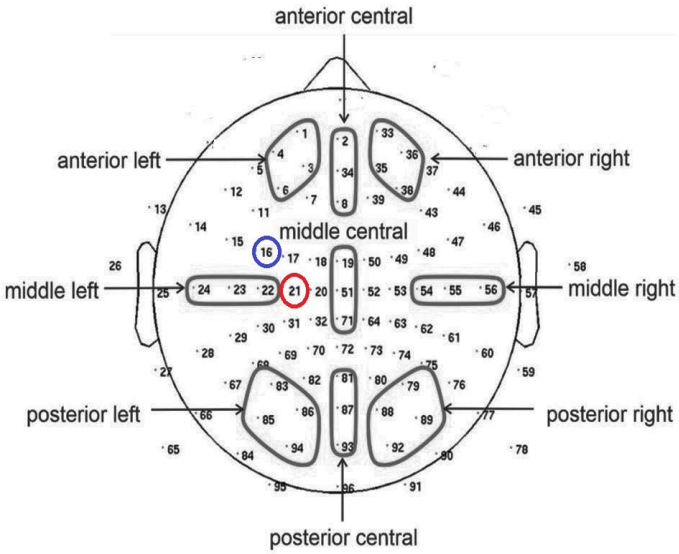

For patient #5: a. The top figure is the original EEG record obtained from the patient. b. The V-TCN identified of a seizure event in the EEG record of an adult male with intractable temporal-lobe epilepsy. The expert-annotated result (shown in blue) is within two electrodes of the result obtained by the system. c. The location of the seizure foci on the EEG montage. The red circle indicates the focus location determined by the V-TCN; the blue circle is the expert determination of the focus

3.3.6 Patient 6: Tonic-Clonic Bilateral Seizure

This data and result are recorded and analyzed from a pediatric male patient with intractable temporal-lobe epilepsy. Two epileptogenic foci were detected, which were found to correspond closely to the expert annotations for this patient data – one, a single electrode off from the expert annotation, the second determined at the same electrode as the expert annotation. Each foci was detected in different hemispheres of the brain, suggesting that one focus might be the primary initiator of the seizure, while the second is entrained through a possible anatomical tract. However, the V-TCN's temporal resolution is not able to specify which focus fired first.

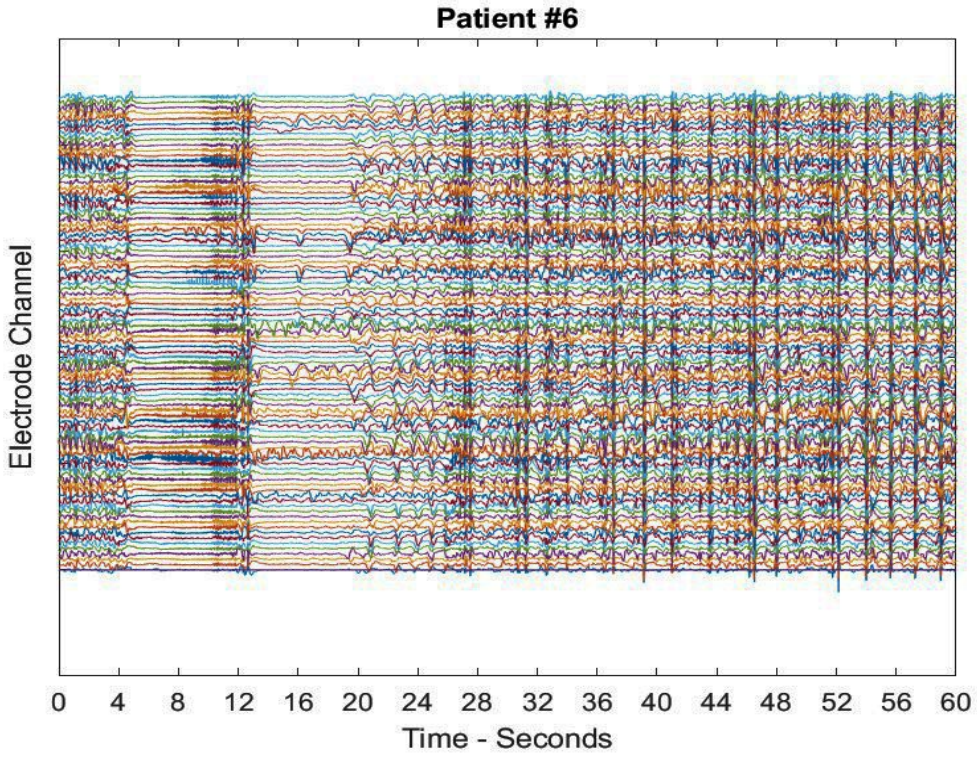

Figure 21. Patient #6

Figure 22. (continued)

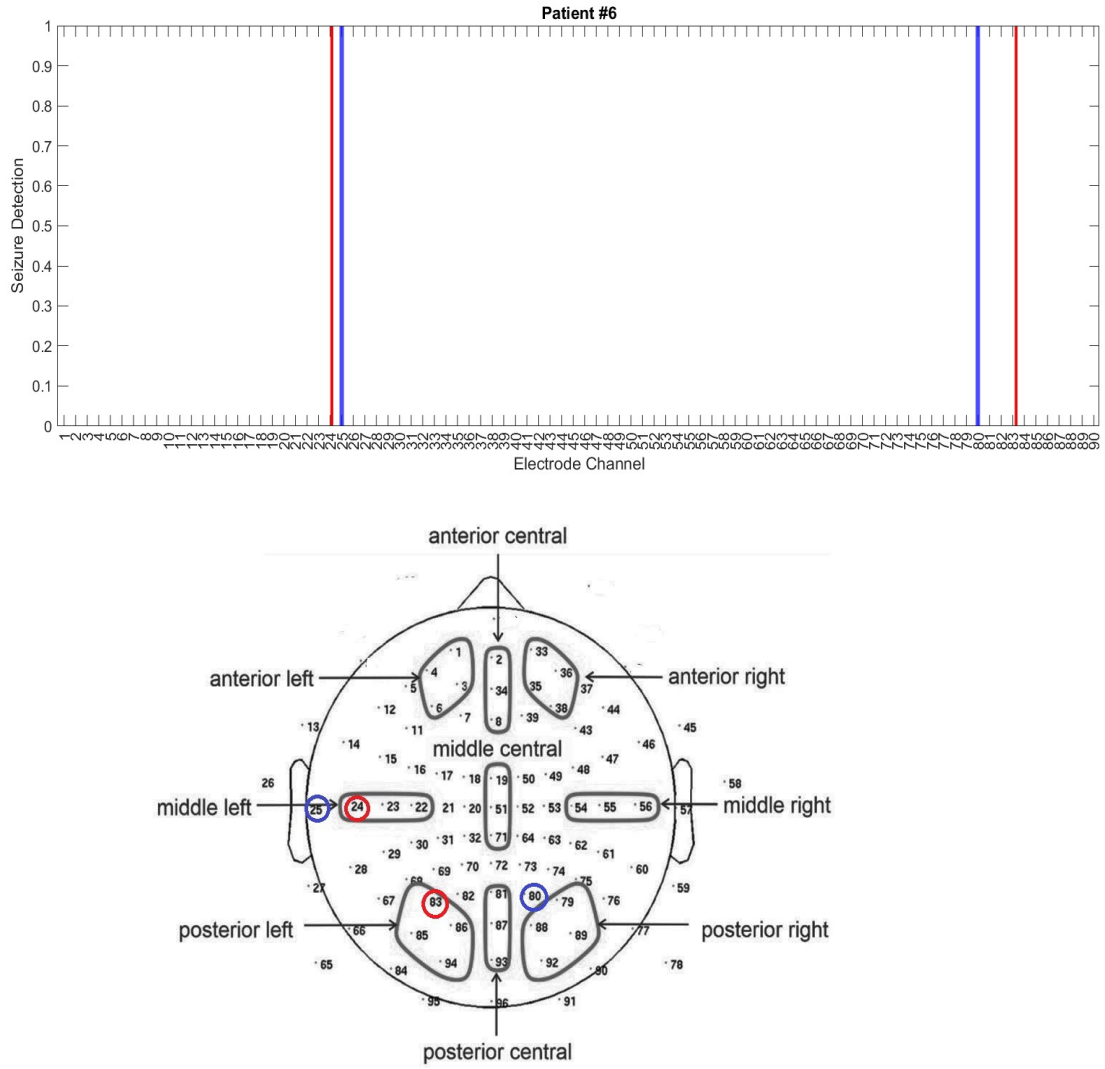

a. The top figure is the original EEG record obtained from the patient. b. The V-TCN identified of a seizure event in the EEG record of an adult male with intractable temporal-lobe epilepsy. The expert-annotated result (shown in blue) is within two electrodes of the result obtained by the system. c. The location of the seizure foci on the EEG montage. The red circles indicate the focus location determined by the V-TCN; the blue circles are the expert determination of the two foci.

3.3.7 Patient 7:

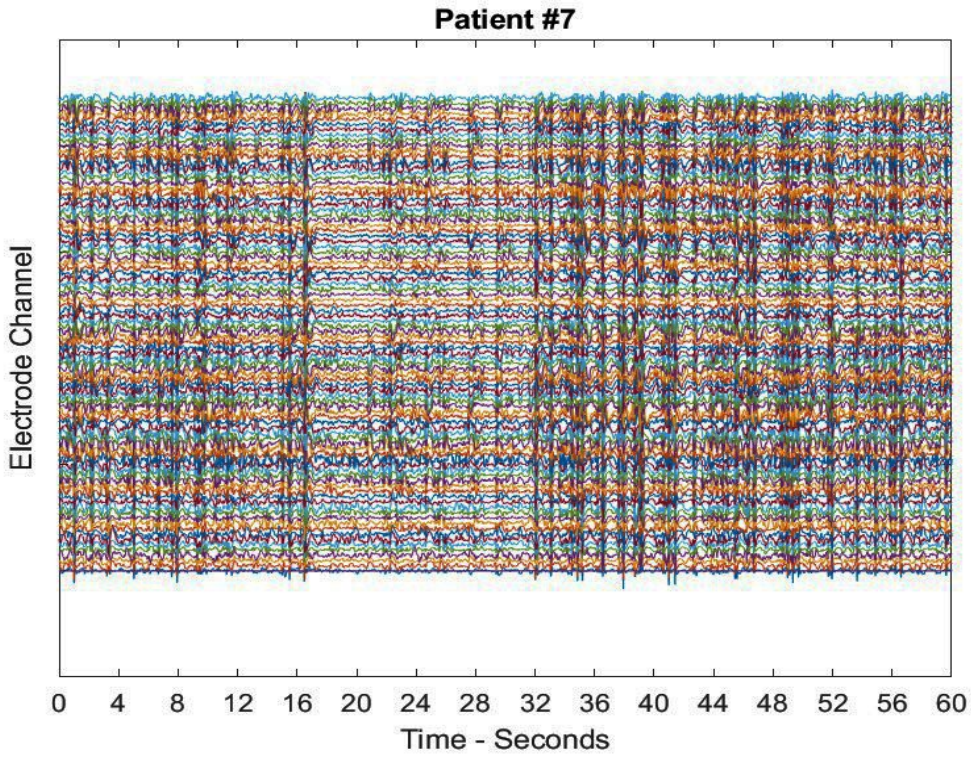

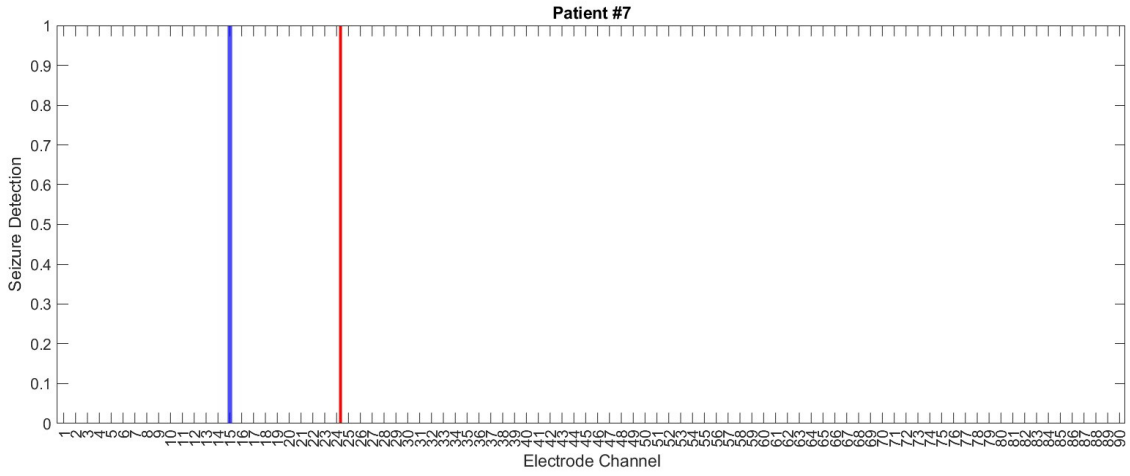

Figure 22. Patient #7

Figure 23. (continued)

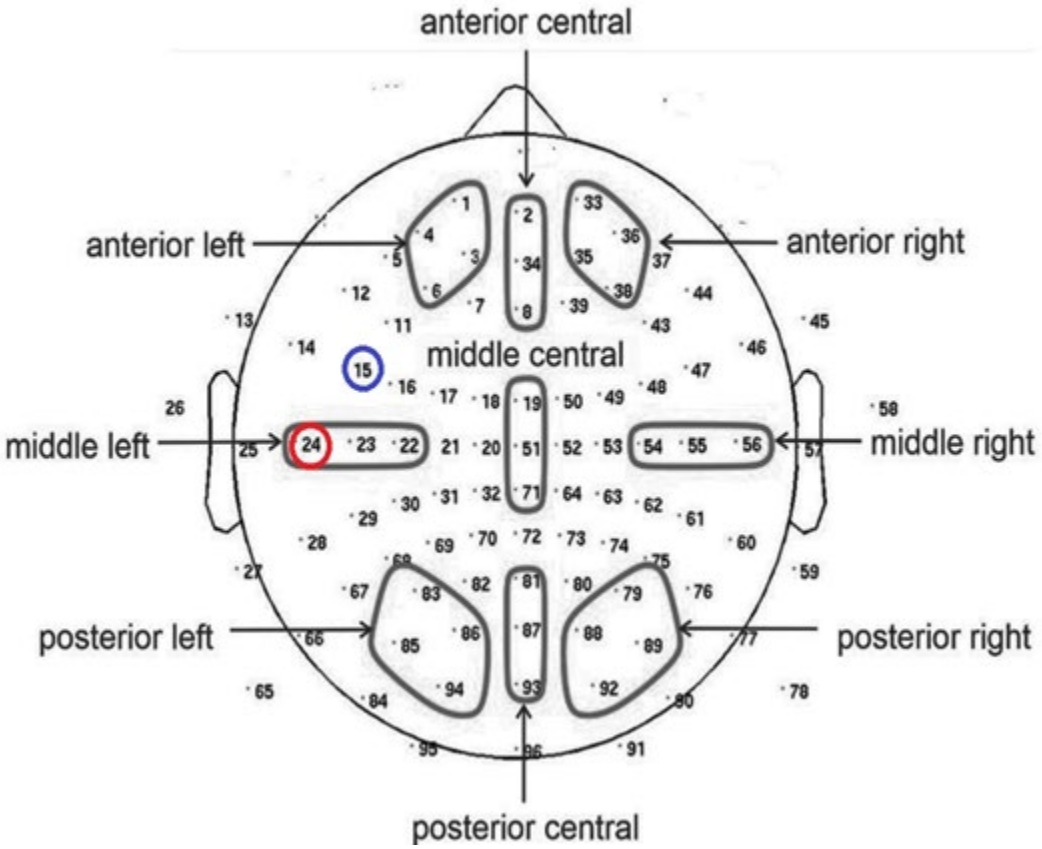

For patient #7: a. The top figure is the original EEG record obtained from the patient. b. The V-TCN identified of a seizure event in the EEG record of an adult male with intractable temporal-lobe epilepsy. The expert-annotated result (shown in blue) is within two electrodes of the result obtained by the system. c. The location of the seizure foci on the EEG montage. The red circle indicates the focus location determined by the V-TCN; the blue circle is the expert determination of the focus

Patient 8

Although there was an expert-annotated seizure event in this EEG record, the V-TCN was not able to correctly detect its presence or specify its location. Various values of the threshold value were tried between 0.85 and 0.95, with no determination of a seizure event. The lack of seizure event detection is a useful true-negative example with which the system can be further trained to the existence of non-seizure data.

Patient 9

This sample also retained a background signal from one of the electrodes not in the 1-90 range and is one of accessory recordings taken while the EEG signal is being recorded from the patient. Again, this was included to see if its presence could greatly affect the T-VCN's ability to detect the seizure event on the correct channel. It's performance was only one electrodes off, an acceptable result within the expected constraints of this study, suggesting that the system can remain unaffected by signals, such as artifacts or supplementary recordings, that are not seizure events.

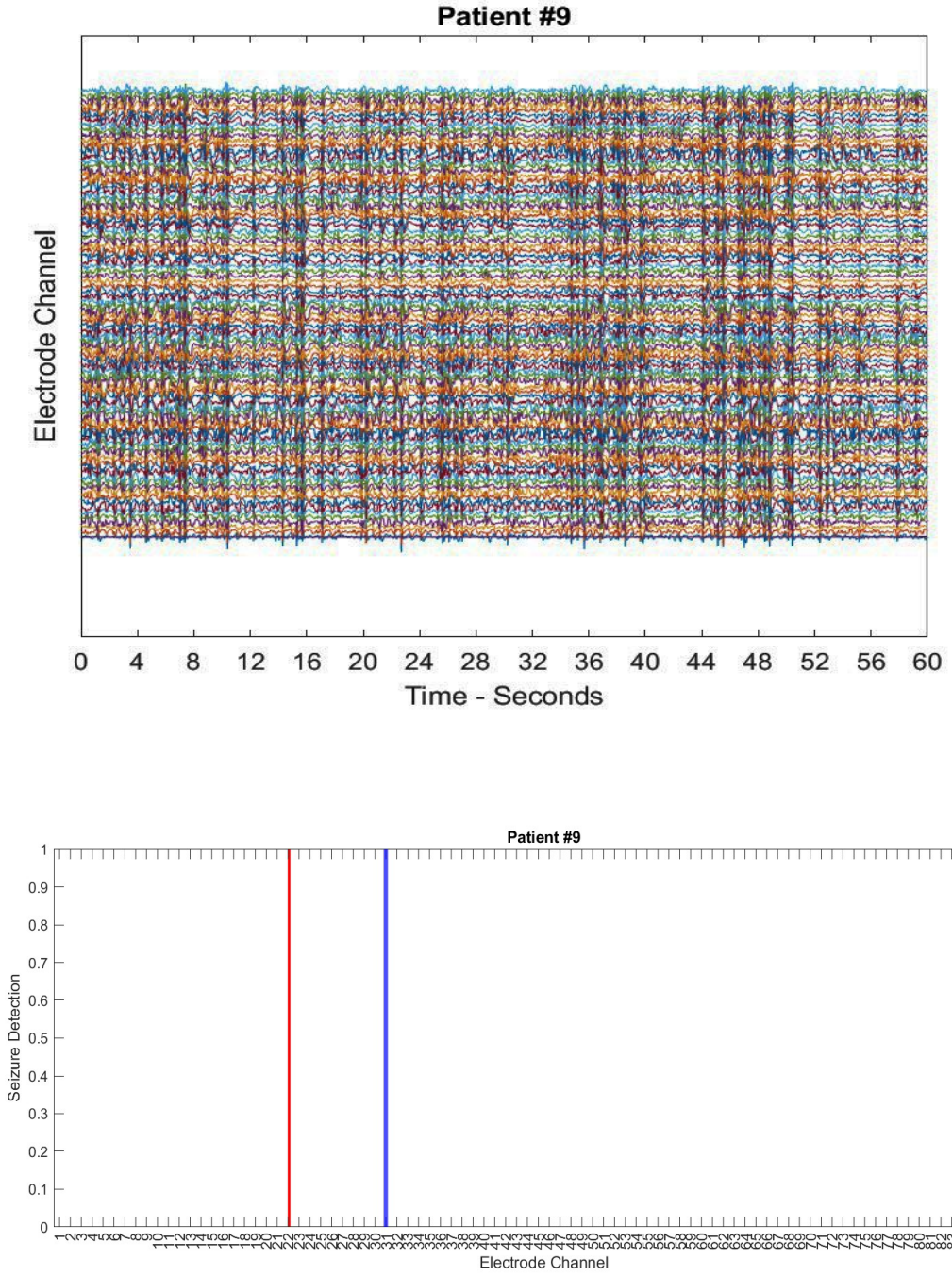

Figure 23. Patient #9

Figure 24. (continued)

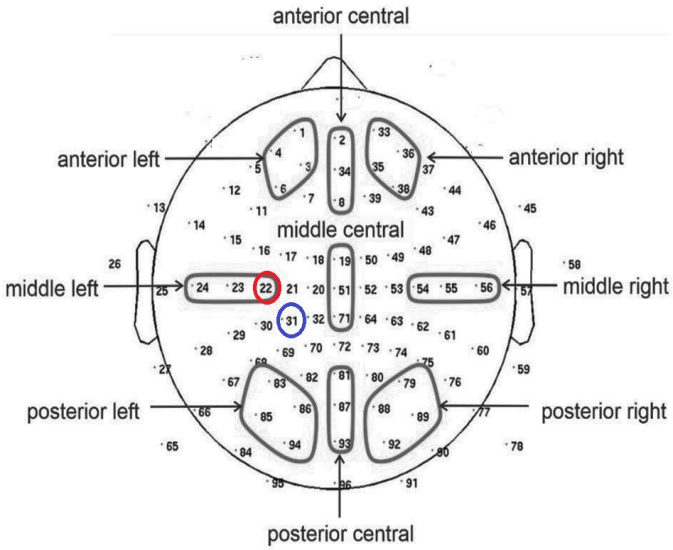

For patient #9: a. The top figure is the original EEG record obtained from the patient. b. The V-TCN identified of a seizure event in the EEG record of an adult male with intractable temporal-lobe epilepsy. The expert-annotated result (shown in blue) is within two electrodes of the result obtained by the system. c. The location of the seizure foci on the EEG montage. The red circle indicates the focus location determined by the V-TCN; the blue circle is the expert determination of the focus

.

3.3.8 Patient 10:

This sample is the third one analyzed that retains a background signal from one of the electrodes not in the 1-90 range. In this case the V-TCN exactly matched the expert determination of the electrode showing the seizure event. The results for patient #10 begin on the following page.

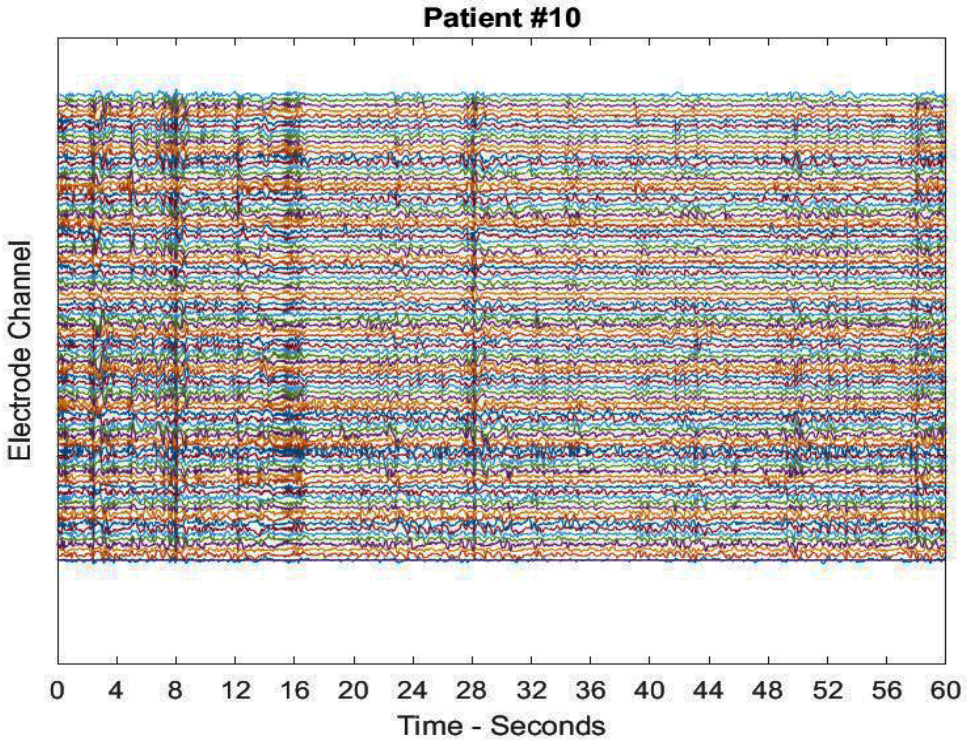

Figure 24. Patient #10

Figure 25. (continued)

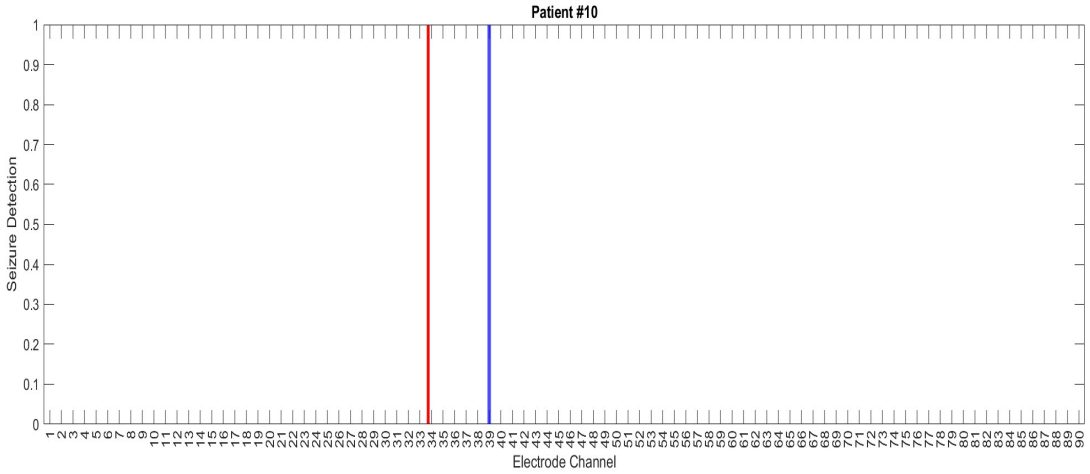

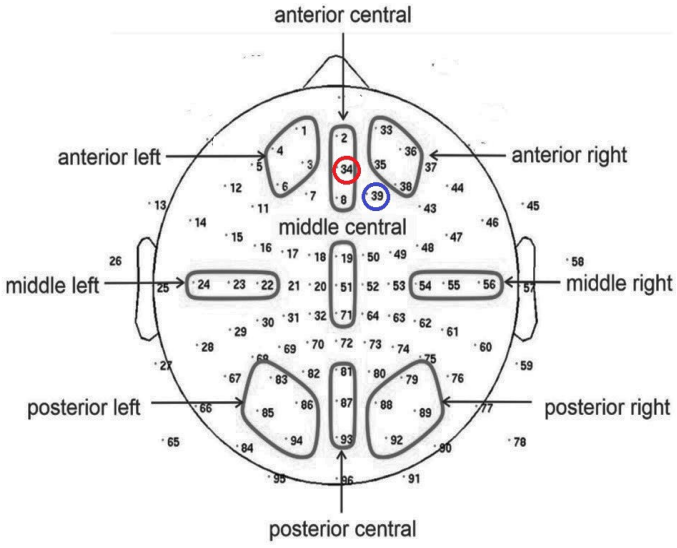

For the final test in this analyses set: a. The top figure is the original EEG record obtained from the patient. b. The V-TCN identified of a seizure event in the EEG record of an adult male with intractable temporal-lobe epilepsy. The expert-annotated result (shown in blue) is within two electrodes of the result obtained by the system. c. The location of the

seizure foci on the EEG montage. The red circle indicates the focus location determined by the V-TCN; the blue circle is the expert determination of the focus

3.3.9 Detection of Time of Seizure Onset

This system was also designed to detect when seizure activity was first detected in the EEG record. This ability was demonstrated in the patient validation set of data. Since the V-TCN tests 4 second partitions of data (according the assumption of stationarity and ergodicity for data samples =< 4 seconds), the partition first showing correspondence to the gold-standard seizure event can be assumed to be the onset of the seizure activity within 4 second accuracy.

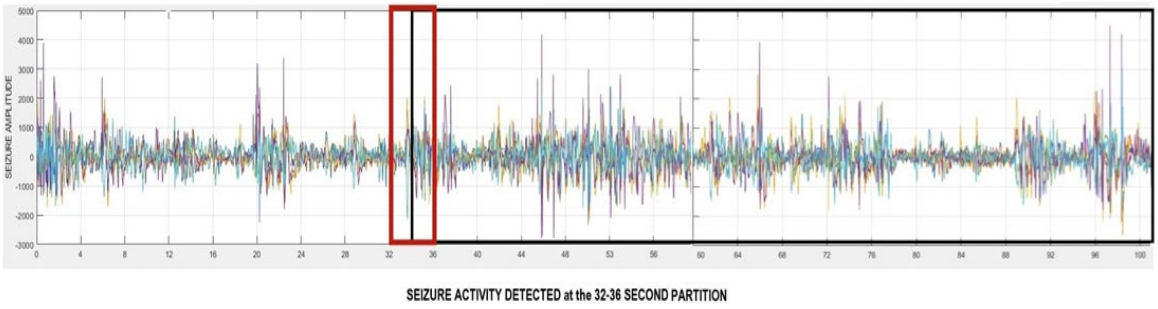

Figure 25. Gold-standard data with the partition containing the epoch at which seizure activity was first detected.

4.0 Discussion

The overall aim of this work is the design of a clinical tool that is useful for clinicians treating seizure-related conditions in patients located in remote, rural, and underserved regions. A deep-learning algorithm is the basis of the system used to analyze short-duration mutli-channel EEG records from patients with intractable epilepsy. The system designed in this study is able to provide a clinician with an approximate cortical location of the seizure focus as well as an approximate time for the seizure onset. The system was designed with various constraints and limitations in mind.

The study of the neuroanatomy and mechanisms of eleptogenessis is still ongoing (Wenzel, Huberfield, Grayden et al., 2023). Similarly, techniques to measure the spatial localization of seizure foci are still under investigation and a variety of solutions have been proposed and tested (Yoganathan, Malek, Torzillo et al. 2023). The methodology and results of many of those studies were considered before the design of the system presented here was undertaken.

There are already established techniques for determining the temporal properties of epileptogenesis. However, due to several factors, spatial localization of the physical site of seizure onset continues to be a difficult goal. This problem largely arises from the loss of the necessary resolution of spatial frequencies during the volume conduction of the cortical signal through the bone and tissues of the head (Srinivasen, Nunez, Silberstein, 1998). Determination of the best montage to overcome this loss is still not a precise technique. In particular, previous work

suggests that the distance between recording scalp electrodes of 20 to 30 mm is necessary to acquire the maximum spatial resolution of an EEG signal (Srinivasan, Tucker, Murias, 1998). It has been reported that montages with as few as 12 channels is sufficient to identify the epileptogenic focus in the cortex (Toth R, Barth A, Domokos A et al, 2021).

Note that in temporal lobe epilepsy remediation surgery, 4 to 5 cm of the brain may be resected (Müller M, Schindler K, Goodfellow M, et al, 2018). Temporal lobe surgical resection can give a patient seizure remission in about 80% the cases but how this kind of surgery affects the structural white matter network, and, therefore, how the network changes relate to seizure outcome remains unclear (Taylor P, Sinha N, Wang Y, 2018).

To achieve the aim of this research – where great precision of spatial localization of seizure foci was not necessary to the intended use of the system in the field, temporal convolutional neural network-based computer utility to determine both the onset time and the cortical localization of seizure foci was designed and tested. High-resolution data from 90-channel EEG data samples were tested in order to test the ability of the system to discriminate seizure onset and foci localization from cortical sites that might be close together.

Scalp electrodes are usually 10 mm in diameter and this sets a hard limit for the accuracy of signal localization. If the recording array consists of a large number of electrodes, such as with this study, there is a likelihood of recording overlap in signal localization. The results from the analyses in this study show that an expert annotated seizure event may appear on an electrode one removed from the electrode detected by the system, which is acceptable given the possibility of signal overlap from the large montage of 90 electrodes.

With these considerations, it is proposed that, especially for field use and using the results of the studies mentioned above, that a smaller scalp electrode array, such as a 32-electrode set up, would be sufficient to approximate seizure focus localization. For purposes other than field recordings in underserved areas, such as in a hospital epilepsy monitoring unity (EMU), depth electrodes can be used for long term EEG recordings that last several hours or more.

The consistency of results obtained from a number of subdural EEG data sets verifies that the Volterra-TCN accomplished what it was designed to do within the bounds of a number of limitations. However, in order to interpret the results realistically, it is necessary to consider them within the context of a number of constraints of the clinical and experimental environments in which they were obtained. These limitations include the nature of the neural network training and test data, the particular complexity of the data used, the restrictions associated with the type of neural network used, and the approximations inherent in the recording techniques.

4.1 Neural Network Limitations

A significant limitation of any computer-based analysis technique is how it performs with respect to problem size and complexity. There are considerable trade-offs between the complexity of the data under consideration and the characteristics of the neural network used to analyze them. In general, the quality of the results obtained from the neural network depends on: (1) the complexity of the data being analyzed and the agreement between experts who determine what constitutes “gold-standard” data, (2) the extent of noise in the training data

resulting from recording techniques, and (3) the size and architecture of the network in relation to the size required for an optimal or clinically acceptable solution.

The assumptions made in this study may be the source of inherent errors that permeate the final and total collections of data:

Since EEG signals are non-stationary, certain assumptions must be considered when considering appropriate sample characterization for study. Considering the EEG signal to be stationary in the strong sense (all moments are equal) over a short time interval (e.g. 4 seconds) is one empirical approximation to the data. By taking a sample of this short duration, one may also consider the signal within this time interval to be stationary over an interval.

Other general assumptions made regarding the unprocessed EEG data are reasonable approximations. In the EEG frequency range, the combination of signals received at the electrodes can be assumed to be linear. Also, during a seizure event, correlated activity in two components occurring in the same time-interval period is not attenuated by other independent activity, including baseline noise. Therefore, periods of correlated activity reflects the emergence of temporarily coupled sources that integrate synchronously active network.

Addressing the second limitation of neural network analysis of EEG, there are a number of approximations introduced into the results by the techniques used to obtain the EEG signals during clinical recordings.

However, certain trends can be taken into account when undertaking an iterative design of the network. In particular, adjustment of the network training rate is one parameter that is readily adjusted within the MATLAB code used to design the neural network. Since the TCN

architecture involves short-term memory, the lag-time in the response of the neural network to abruptly changing patterns (viz. from non-seizure-like to seizure-like) must be considered. For the architecture used in this study, one iteration of the network represented $1/250^{th}$ of a second (the sampling rate), so the total lag-time of this particular network was considered to be insignificant.

The training algorithm itself, the resilient back-propagation algorithm, is not typically used to train recurrent neural networks. The most widely-used gradient-based algorithms for training these type of networks are the backpropagation-through-time, recurrent backpropagation, and real-time recurrent learning algorithms. However, these algorithms tend to be affected by slow convergence. Most backpropagation algorithms are restricted by the potential problem resulting from the weight changes being a function of the gradient magnitude. Since the resilient backpropagation algorithm employs only the sign of the derivative to specify the direction of weight update, the potential problem arising from the increasing magnitude of the weight step partial derivative is avoided. This results in a typically quicker training time. Since the ultimate goal of this project is to provide a clinically useful utility, a relatively rapid training time is preferred.

A consequence of using a rapid training algorithm is the benefit of being able to specify a low learning goal – one that does not require a long training time to reach. For point (2), network overfitting can result in lower training and generalization error in certain cases.

4.2 Data Recording Limitations

Only data from male patients were analyzed in this study. However, gender differences in epileptic patients have been noted in other research. In particular, no gender differences were noted in localization-related epilepsy (LRE). However, more specifically, symptomatic LREs (where the seizure origin was detected in a localized region of the brain) were seen to be more frequent in men, whereas women presented with more frequent cryptogenic LREs (seizures of unknown etiology) (Christensen J, Kjeldsen M, Andersen H, Friis M, Sidenius P, 2005). Therefore, future work with the technology developed here needs to include a broader selection of data that includes female subjects.

The primary characteristics of recorded EEG signals are greatly affected by the physiological environment from which they are obtained. If these signals are derived from scalp measurements, they are highly attenuated by the skull and spatially filtered in the low-pass range. Even electrodes which are placed subdurally may be receiving signals attenuated by brain tissue, even though subdural signals may yield more information if an optimal number of electrodes are used. It has been shown that the more invasive electrode placements yield a higher resolution of a seizure event but a corresponding lower maintenance of stability over time (Slutzky M, Jordan L, Krieg T et al, 2010). The data obtained for this study was all scalp recorded data. This is in accordance with the project requirement that the system be able to function in the field with relatively basic recording equipment. Studies have shown that 19-electrode recordings have optimal spatial resolution around 22-37 cm^3 and a 129-electrode montage can provide a resolution about 6-8 cm^3 (Feree T, Clay M, Tucker D, 2001).

There is a continuing discussion on the optimal placement as well as the spacing between the recording electrodes. It has been reported that, in general, the more electrodes used

The electrodes used to obtain EEG signals are very sensitive to the orientation of the brain tissue – thus, there is a selective sensitivity over the entire electrode montage. It is possible for electrodes not in sequence to each other to be situated on the same equipotential line and record a summation of the activity over a wide range of the cortex.

Cortical networks are not physically isolated from one another, nor do they act completely independently. Therefore, the signal received at each electrode is spatially correlated since it represents an ensemble of measurements received from many cortical sources. In the bilateral clonic-tonic seizure examples seen in the results section may be explained by considering that the seizure initiates at one site and activates a secondary site distant to the primary site. This anomaly can be explained by the presence of patient-specific cortical structures that form a epileptogenic networks. At this time, there is not a lot of information on how structural network abnormalities across the brain differ between patients with focal to bilateral tonic–clonic seizures – a possible topic of further research using the techniques described in this study.

Capacitative coupling between electrodes can also introduce artifacts into the recording, since the residual potentials resulting from electrode imperfections are not always stable and are subject to random fluctuation. The charge distribution of an electrode not only introduces a spurious voltage, it can also produce a local capacitance that results in a significant artifact in the EEG recording.

It follows from the issues described above that electrical activity in the brain can overlap others, so that a recording from a single electrode in the brain with respect to some suitable reference point could reflect the activity at many different sites. Thus, the distance between one active cell and the recording site can play a major role in determining the amount of contribution of that particular focus to the total recorded activity. Also, the electrode might lie on or near the zero isopotential surface of the epileptogenic focus and, therefore, record little or no activity, even if that focus be adjacent to the electrode. This problem is not solved by bipolar recording, because both electrodes might reside on the same isopotential of the field. Neurons arranged in symmetrical layers or columns, characteristic of cortical and other laminar structures, provide a geometric basis for the addition of sources and sinks and can show greater amplitudes of electrical activity than other structures.

In addition, distinct populations of cortical neurons may be interconnected in the cortical laminar structure. In such a case, their electrical activity might overlap to some extent and the signals derived from such distinct populations can be similar in their frequency components and amplitudes, making the separation of each signal source from such populations very difficult -- especially when the goal is to record the spontaneous changes that characterize ictal events. A solution to this problem may not be currently available, no matter how many recording electrodes are used. Furthermore, the recordable signal generated by the focus propagates across the cortical field and the actual focus of seizure origin may be difficult to isolate once the seizure has initiated.

At this time, this system cannot distinguish pre-seizure onset signals from fully-developed seizure signals. Collection and testing of gold-standard data that has expert specified epochs of pre-seizure data would be required to extend the resolving capacity of the current utility.

5.0 Conclusions

It was shown successfully that a temporal convolutional neural network with a Volterra kernel and a relatively simple architectures is capable of detecting seizure-like activity in multi-channel EEG records. Furthermore, the results obtained from the three different architectures studied were fairly consistent in locating the generators of seizure-like activity based on the patient's subdural EEG montage. If these results are verified by other studies, then these neural networks may serve as effective functional engines in more sophisticated seizure detection utilities. Additional work to increase the detection ability of these networks needs to be undertaken, especially with regard to the separation of the EEG data recorded at each electrode. Also, a means by which a utility using these neural networks can be made more adaptive to a variety of seizures from a wide patient population needs to be examined.

Despite the initial success of this utility in detecting and localizing seizure activity in epilepsy patients, several important tasks remain.

Additional testing must be done – and some previous results retested – after several techniques for network weight resetting are considered. The software clears the program cache on each run of the utility, but the weights remain fixed from the previous test. To ensure that the network can generate accurate results, the weights must be reset for each new data run. There are several techniques for resetting weights than can be considered, such as Weights Reset, Xavier initialization, He-et-al Initialization, etc.

This utility was tested only on patients with temporal lobe epilepsy. To be considered a

truly versatile tool for clinicians in the field, especially those health-care providers who do not possess neurodiagnostic expertise, this tool must be able to handle EEG recordings from patients with a wide variety of medical issues, both physical and physiological, such as traumatic brain injuries and drug overdoses. If, even constructing a versatile library of seizure detection results from a number of patients, the utility must be able to handle exceptions and notify the clinician that an unknown event has been detected instead of providing false conclusions of the seizure time-onset and cortical localization. To achieve this ongoing goal, additional testing with data from patients with a variety of medical concerns must be included in the analyses.

A user-friendly interface needs to be designed and constructed to allow a first-time user or an inexperienced clinician the ability to quickly understand and utilize the complete functionality and limitations of the software. The menus must be understandable by emergency medical personnel as well as skilled neurosurgeons. To that end, testing the utility with a wide variety of user is necessary.

At this time, the software, written entirely in MATLAB and currently in a development stage must be completed according to the standard required by the IEC 62304 standard, a medical industry norm. This standard is typically completed in association with IEC 13485. The quality management system for medical devices. Validation and verification protocols need to be included in the revision of the software as it is redesigned to meet the above standards.

A current post-PhD project currently being considered is the design of an entire EEG recording kit to be employed in the field. This complete kit consists of a rugged laptop, specifically designed for use in outside use, such as the Lenovo ThinkPad X1 Carbon Gen 11 or

Dell Latitude 7330 Rugged Laptop, to run the finalized version of the software. For initial field testing, a sixteen-channel EEG recording headset, such as the OpenBCI Ultracortex EEG headset and Cyton/Daisy bioamplifier, is currently being considered.

The system developed in this research demonstrated that a relatively simple, but carefully designed and properly trained, machine learning algorithm is useful in detecting seizure activity in epilepsy patients. Further development and field testing of this system can be used to demonstrate its utility in detecting seizure activity in patients with other trauma affecting the brain, especially traumatic brain injuries. This system could be particularly useful in streetside applications where emergency personnel can quickly detect the presence of seizure activity caused by brain injury. Even without precisely localizing the seizure focus (or foci), the presence or lack of detected seizure propagating injuries can be a useful diagnostic for clinicians receiving the patient in the emergency department.

6.0 Appendix

6.1 Development of the Volterra Kernel for the TCN: Volterra Representation of the Montage with Two-Dimensional Spatial Convolutions

The advantage of using a Volterra series is that it converges for most nonlinearities, except very large input values or nonlinearities of very high order – constraints which do not affect this current study [Marmarelis p 245].

These terms are the basis for expressing the discrete Volterra series expansion for the input-output relation of a discrete-time causal, nonlinear, time invariant system, which is given by:

y(n) =

$$k_0 + T\sum_{m_1=0}^{M} k_1(m_1)x(n-m_1) + T^2\sum_{m_1=0}^{M}\sum_{m_2=0}^{M} k_2(m_1m_2)\times x(n-m_1)x(n-m_2)+\ldots \quad \text{(A-1)}$$

where:

x(n) is the input sequence of data,

y(n) is the output sequence,

M is the finite memory of the system, which corresponds to the input epoch values,

$x_{n,m}$ = x(n-m) at each time n,

T is the sampling interval,

k_i are the Volterra kernels.

The kernel functions $\{w_i\}$ fully characterize the nonlinear input-output mappings of the system and so describe the nonlinear dynamics of the system [.

With these limitations in mind, the following Volterra model is derived for a two-dimensional spatial representation of the EEG montage:

$$y(n) = \sum_{i=0}^{M} \sum_{m_1,\ldots,m_i} k_i\,(m_1,\ldots,m_i)x(n-m_1)\ldots x(n-m_i) \qquad \text{(A-2)}$$

where:

x(n) is the electrode index:

n = 0: central electrode,

n = 1: nearest neighbor electrode in the montage,

n = 2: next-nearest neighbor electrode in the montage.

where:

y(n) is the system output,

k_i are the kernel functions of that describe the nonlinear dynamics of the system,

m_i, n_i are discrete spatial indices,

M represents the electrode "neighborhood" consisting of an electrode and its nearest neighbors and next-nearest neighbors.

This Volterra model consists of a series of functional terms which map the signal from a particular set of electrodes [n, n – M] to the output value y(n):

$$k_0 + T\sum_{m_1=0}^{M} k_1(m_1)x(n-m_1) + T^2\sum_{m_1=0}^{M}\sum_{m_2=0}^{M} k_2(m_1m_2)\times x(n-m_1)x(n-m_2)+\ldots$$

(A-3)

such that:

$$y(n) = \underbrace{k_0}_{central-electrode} + \underbrace{\sum_{m_1=0}^{2} k_1(m_1)x(n-m_1)}_{nearest-neighbor}$$

$$+ \underbrace{\sum_{m_1=0}^{2}\sum_{m_2=0}^{2} k_2(m_1,m_2)x(n-m_1)x(n-m_2)}_{next-nearest-neighbor}$$

(A-4)

This finite Volterra series is equivalent to the multinomial power series expansion of a nonlinear function given by:

$$y(n) = F(x_{n,0}, x_{n,1}, x_{n,2}) \quad \text{(A-5)}$$

where, as above, the M+1 = 3 arguments of the function F correspond to the input spatial values of the montage:

$$x_{n,m} \equiv x(n - m) \text{ for each sample time } t \quad \text{(A-6)}$$

The second functional term of the equation above [#], representing the next-nearest neighbor values of the montage, is a two-dimensional convolution involving spatially shifted neighbors of the central electrode [n, n – 2] and the second order kernel k_2.

Continuing with the methodology designed by Marmarelis, the kernels can be expanding on an orthonormal basis $\{b_j(m)\}$over the interval [0,2]. The Volterra series can then be

represented as follows:

$$y(n) = c_0 + \sum_j c_1(j) v_j(n) + \sum_{j_1} \sum_{j_2} c_2(j_1, j_2) v_{j1}(n) v_{j2}(n) \quad \text{(A-7)}$$

where:

$$v_j(n) = \sum_{m=0}^{2} b_j(m) x(n-m) \quad \text{(A-8)}$$

which is simply a weighted sum of the input electrode values up to the next-nearest neighbors in the montage.

and:

c_0, c_1, c_2 are the kernel expansion coefficients (Note that $c_0 = k_0$),

b_j are the basis functions.

The nodes of the hidden layer use polynomial activation functions instead of the typical sigmoidal functions. This renders the network functionally equivalent to a Volterra model [Mitsis p 280].

Thus, the input of the kth hidden unit is given by:

$$u_k(n) = \sum_{i=0}^{2} \sum_{j=0}^{2} w_{kj}^{i} v_j^i(n) \quad \text{(A-9)}$$

The output of the hidden layer is then given by:

$$z_k(n) = \sum_{m=0}^{2} c_{m,k} u_k^m(n) \quad \text{(A-10)}$$

and the network output is given by:

$$y(n) = \sum_{k=0}^{4} z_k\,(n) + y_0 \text{ for five nodes in the hidden layer} \qquad \text{(A-11)}$$

With this Volterra formalism in place, the architecture of the Volterra neural network used in this study can be designed.

7.0 Bibliography

Acharya J, Acharya V. 2019. Overview of eeg montages and principles of localization. *J Clin Neurophys*. 36(5): 325-329.

Acharya U, Sree S, Swapma G, Martis R, Suri J. 2013. Automated EEG analysis of epilepsy: a review. *Knowledge-Based Systems*. 147-165.

Aloitaiby T, Samie F, Alshebeili S, Ahmad I. 2015. A review of channel selection algorithms for eeg signal processing. *J Adv Sig Proc*. 2015(66): 1-21.

Artoni F, Delorme A, Makeig S. 2018. Applying dimension reduction to eeg data by principal component analysis reduces the quality of its subsequent independent component decomposition. *Neuroimage* 175, 176-187.

Askham, A. 2023. Brain imaging do-over offers clues to field's replication problem. *Spectrum: autism research news*. https://doi.org/10.53053/NUDA6617.

Bai S, Kolter J, Koltun. 2018. An empirical evaluation of generic and recurrent networks for sequence modeling. *arXiv*:1803.01271v2.

Banarjee M, Chakraborty R, Bouza J. VolterraNet: a higher-order convolutional network with group invariance for homogenous manifolds. *IEEE Trans Pattern Analy and Machine Intel*. 30(30): 1-11.

Bartolomei F, Cosandier-Rimele D, McGonigal A, Aubert S, Regis J, Gavaret M, Wendling F, Chauvel, P. 2010. From mesial temporal lobe to temporoperisylvian seizure networks. *Epilepsia*. 51(10): 2147-2158.

Basavarajaiah D, Murthy, B. 2020. Applications of machine learning in medical research. In: Design of Experiments and Advanced Statistical Techniques in Clinical Research. Singapore Springer. 157-178.

Bates R [Mackenzie R] Sun M, Scheuer M, Sclabassi R. Seizure detection by recurrent neural network. Biomedical Engineering: Recent Developments. J Vossoughi (Editor), Medical and Engineering Publishers, Inc. 139-60.

Bates R [Mackenzie R]. 2001. Detection of seizure foci by recurrent neural networks. University of Pittsburgh: MS Thesis.

Baumgartner C, Koren J, Britto-Arias M, Zoche L, Pirker S. 2019. Presurgical epilepsy evaluation and epilepsy surgery. *F1000 Res*. 1-13.

Bednarski B, Singh A, Zhang W. 2022. Temporal convolutional networks and data rebalancing for clinical length of stay and mortality prediction. *Sci Reports* 12:21247.

Beniczky S, Schomer D. 2020. Electroencephalography: basic biophysical and technological aspects important for clinical applications. *Epileptic Disord* 22(6): 697-715.

Bernhardt C. 2017. Turing's vision: the birth of computer science. MIT Press.

Bertram E. 2014. Electrophysiology in epilepsy surgery: roles and limitations. *Ann Indian Acad Neurol* 17:540-4.

Birpoutsoukis G, Csurcsia P, Schoukens J. 2018. Efficient multidimensional regularization for volterra series estimation. *Mech Sys Sig Proc* 104: 896-914.

Bitbrain, 2020. How deep learning is changing machine learning ai in eeg data processing. https://www.bitbrain.com/blog/ai-eeg-data-processing.

Borck C. 2018. Brainwaves: a cultural history of electroencephalography (science, technology and culture, 1700-1945) Routledge.

Boyd S, Chua L. Fading memory and the problem of approximating operators with volterra series. *IEEE Trans Circ Sys*. CAS-32(11): 1150-1161.

Boyd S, Tang Y, Chua L. 1983. Measuring volterra kernels. IEEE Trans Circ Sys 30[8]: 571-577.

Branco M, Geukes S, Aarnoutse E, Ramsey N, Vansteensel M. 2022. Nine decades of electrocorticography: A comparison between epidural and subdural recordings. *Europe J. Neurosci*. 1– 29.

Brock J, Abdallah Z. 2022. Investigating temporal convolutional neural networks for satellite image time series classification. *arXiv*:2204.08461v1.

Budura G, Botoca C. 2005. Nonlinear identification using the lms volterra filter. *Proc 2005 WSEAS Intr Conf Dynam Sys Control* Nov: 148–153.

Burle B, Spieser L, Roger C, Casini L, Hasbroucq T, Vidal F. Spatial and temporal resolutions of eeg: is it really black and white? a scalp current density view. *Intl J Psychophysiol*. 97: 210-220.

Cascino G, Brinkmann B. 2021. Advances in the surgical management of epilepsy. *Neurologic clinics*, 2021. 39 (1): 181-196.

Casson A. 2019. Wearable eeg and beyond. *Biomed Engr Letters* 9: 53-71.

Chang E. 2015. Epileptogenic zone localization using magnetoencephalography predict seizure freedom in epilepsy surgery. *Epilepsia* 56(6): 949-958.

Christensen J, Kjeldsen MJ, Andersen H, Friis ML, Sidenius P. Gender differences in epilepsy. *Epilepsia*. 2005 Jun;46(6):956-60

Connolly M, Sharbrogh F, Wong P. 2003. Electrical fields and recording techniques in Ebersole J, Pedley (eds) Current practice of clinical electroencephalography. Philadelphia: Lippincott Williams and Wilkins, 72-99.

Craley J, Johnson E, Venkataraman A. 2020. A spatio-temporal model of seizure propagation in focal epilepsy. *IEEE Trans Med Imaging* 39(5):1404-1418.

Culler G, Jobst B. 2022. Surgical treatments for epilepsy. *Epilepsy* 8(2): 536-558.

Dai J, Li Y, He Kaiming. 2016. R-FCN object detection via region-based fully convolutional networks. *arXiv:*1605.06409v2.

Emami A. Kunii N, Matsuo T. 2019. Seizure detection by convolutional neural network-based analysis of scalp electroencephalography plot images. NeuroImage: Clin 22(101684): 1-10.

Englot D, Nagarajan S, Imber B, Raygor K, Honma S, Mizuiri D, Mantle M, Knowlton R, Kirsch H,

Fan, Y, Yu R, Li, J. 2020. EEG-based mild depression recognition using multi-kernel convolutional and spatial-temporal feature*. 2022 Intl Conf Biomet and Biomed*: 1777-1784.

Fauser S, Schulze-Bonhage A. 2004. How large must an epileptic focus be to cause an eletrographic status epilepticus – a case report. *Clin Neurophy* 115: 2274-2279.

Feree T, Clay M, Tucker D. 2001. The spatial resolution of scalp eeg. *Neurocomp* 38-40: 1209-1216.

Furui A, Onishi R, Takeuchi A, Akiyama T, Tsuji T. 2021. Non-gaussianity detection of eeg signals based on multivariate scale mixture model for diagnosis of epileptic seizures. *IEEE Trans Biomed Eng* 68(2):515-525.

Gao Y, Gao B, Chen Q. 2020. Deep convolutional neural network-based electroencephalogram (eeg) signal classification. Frontiers Neurology 11(375): 1-11.

Gevins A, Yeager C, Diamond S, Spire J, Zeitlin G, Gevins 1975. A. Automated analysis of the electrical activity of the human brain. *Proc IEEE* 63(10): 1382-1399.

Gonen F, Tcheslavski. 2012. Techniques to assess stationarity and gaussianity of eeg: an overview. *Int J Bioinform* 16(2): 136-142

Gotman J, Gloor P. 1976. "Automatic Recognition and Quantification of Interictal Epileptic Activity in the Human Scalp EEG," Electroenceph. and Clin. Neurophys., 41: 513 – 529.

Gotman J, Ives J, Gloor P. 1979. Automatic recognition of inter-ictal epileptic activity in prolonged eeg recordings. Electroencephalogr Clin Neurophysiol 46(5): 510-520.

Gotman J. 1982. "Automatic Recognition of Epileptic Seizures in the EEG." *Electroenceph. and Clin. Neurophys*. 54: 530-540.

Gugerty L. 2006. Newell and simon's logic theorist: historical background and impact on cognitive modeling. *Proc Human Factors* 50(9): 880-884.

Harpale V, Bairagi V. 2016, Time and frequency domain analysis of EEG signals for seizure detection: A review. IEEE 2016 Intl conf microelectronics comp comm. 1-6.

Haykin, S. 1999. Neural networks: a comprehensive foundation. Upper Saddle River: Prentice-Hall.

Hebb D. 1949. The organisation of behaviour. New York, NY: John Wiley and Sons.

Ide H, Kurita T. 2017 Improvement of learning for cnn with relu activation by sparse regularization. 2017 *Inter Joint Conf Neural Networks (IJCNN)*. 2684-2691.

Israelsen B, Smith Dale. 2014. Generalized laguerre reduction of the Volterra kernel for practical identification of nonlinear dynamic systems, Corr abs/1410.0741.

Jiruska P, de Curtis M, Jeffreys J, Schevon J, Schiff S, Schindler K. 2013. Synchronization and desynchronization in epilepsy: controversies and hypothesis. *J Physiol* 591(4); 787-797.

Kaculini C, Tate-Looney A, Seifi A. 2021. The history of epilepsy: from ancient mystery to modern misconception. *Cureus* 13(3):1-6.

Kaiboriboon K, Bakaki P, Llatoo S, Karoukian S. 2013. Incidence and prevalence of treated epilepsy among poor health and low-income americans. *Neurology* 80(21):1942-1948.

Kandel E, Schwartz J, Jessell T. 1991. Principles of neural science. New York: Elsevier Science Publishing Co., Inc.

Kappel S, Looney D, Mandic D, Kidmose P. 2017. Physiological artifacts in scalp eeg and ear eeg. *Biomed Eng Online* 16(103): 1-16.

Koren J, Herta J, Furbass F, Pirker S, Reiner-Deitmeyer V, Riederer F, Flechsenher J, Hartmann M, Kluge T, Baumgartner C. 2018. Automated long-term eeg review: fast and precise analysis in critical care patients. *Front Neurol*. 2018; 9: 454.

Krizhevsky A, Sutskever, I, Hinton, G. 2017. "ImageNet classification with deep convolutional neural networks". *Comm ACM*. 60 (6):84–90

Lea C, Flynn M, Vidal R, Reitner A. Hager G. 2017. Temporal convolutional networks for segmentation and detection. *IEEE Conf Comp Vision Pattern Recog*. 1003-1012.

Lea C, Vidal R, Reiter A. 2016. Temporal convolutional neural networks: a unified approach to action segmentation. *ECCV Workshops, part III, LNCS* 9915: 47-54.

LeCun Y, Bottou L, Bengio Y, Haffner P. 1998. Gradient-based learning applied to document recognition. *Proc IEEE* 86(11): 2278-2324.

Li T, Zhou G, Qiu Y, Zhao Q. Toward understanding convolutional neural networks from volterra convolution perspective. *J. Machine Learn. Res*. 23(2022): 1-50.

Li T, Zhou G, Qiu Y. 2022. Toward understanding convolutional neural networks from volterra convolution perspective. *J. Machine Learn*. 23: 1-50.

Liang w, Pei, H, Cai Q, Wang Y. 2020. Scalp eeg epileptogenic zone recognition and localization based on long-term recurrent convolutional neural network. *Neurocomputing* 396: 569-576.

Libera A, Carli R, Pillonetto G. 2021. Kernel-based methods for volterra series identification. *Automatica* 129: 1-11.

Lillicrap T, Marblestone A, Olshausen B, Pouget A, Savin C, Sejnowski T, Simoncelli E, Solla S, Sussillo D, Tolias A, Tsao D. Catalyzing next-generation artificial intelligence through neuro ai. arXiv preprint arXiv:2210.08340.

Lim M. 2018. History of ai winters. https://www.actuaries.digital/2018/09/05/history-of-ai-winters/ .

Lindsay, G. 2020. Convolutional neural networks as a model of the visual system: past, present, and future." *J Cog Neurosci* 33: 2017-2031.

Lopes da Silva F, EEG analysis: theory and practice in Niedermeyer E, Lopes da Silva 2005 Electroencephalography: basic principles, clinical applications, and related fields. Lippincott, Williams and Wilkins, 1199-1231.

Loza, C.A., Principe, J.C. (2021). EEG Models and Analysis. In: Thakor, N.V. (eds) Handbook of Neuroengineering. Springer, Singapore. https://doi.org/10.1007/978-981-15-2848-4_65-1

Mani J. 2014. Video electroencephalogram telemetry in temporal lobe epilepsy. *Ann Indian Acad Neurol* 17:s45-9.

Marmarelis V (ed). 1994. Advanced methods of physiological system modeling vol 3. Plenum Press

Marmarelis V. 2004. Nonlinear dynamic modeling of physiological systems. IEEE Press Series in Biomed Engrg, 29-66.

McCorduck, P. 1979. Machines who think: a personal inquiry into the history and prospects of artificial intelligence. New York: W.H. Freeman.

McIntosh WC, M Das J. Temporal Seizure. *StatPearls* [Internet]. Treasure Island (FL): StatPearls Publishing; 2023 Jan-. Available from: https://www.ncbi.nlm.nih.gov/books/NBK549852/

Michel C, Brunet D. 2019. EEG source imaging: a practical review of the analysis steps. *Frontiers Neurol*. 10(325):1-17.

Mitsis G, Marmarelis V. 2002. Modeling of nonlinear physiological systems with fast and slow dynamics: I methodology. *Ann Biomed Engr* 30:272-281.

Mlinar S, Petek, D, Cotic, Z, Ceplak M, Zaletel M. 2016. Persons with epilepsy: between social inclusion and marginalization. *Behav Neurol* 2016:2018509.

Monif M, Seneviratne U. 2017. Clinical factors associated with the yield of routine outpatient scalp electroencephalograms: A retrospective analysis from a tertiary hospital. *J Clin Neurosci*. 45:110-114.

Müller M, Schindler K, Goodfellow M, Pollo C, Rummel C, Steimer A. Evaluating resective surgery targets in epilepsy patients: A comparison of quantitative EEG methods. *J Neurosci Methods*. 2018 Jul 15;305:54-66.

Nettinga, J., Naseem, S., Yakobi, O. et al. 2024. Exploring EEG resting state as a function of boredom proneness in pre-adolescents and adolescents. *Exp Brain Res* 242, 123–135.

Nickels K, Wong-Kisiel L, Moseley B, Wirrell E. 2012. Temporal lobe epilepsy in children: review article. *Epilepsy Research and Treatment*. 1-16.

Nicoletti A, Giuliano L, Colli C, Cicero C, Padilla S, Vilte E, Mayaregua D, Martinez M, Camargo M, Zappia M, Bartoloni A, Gómez E. Treating people with epilepsy in rural low-income countries is feasible. observations and reflections from a "real life experience" after a long lasting intervention in the rural chaco *Front Neurol*. 2018 Oct 10;9:855

Nirthika R, Manivannan S, Ramanan A. 2022. Pooling in convolutional neural networks for medical image analysis: a survey and empirical study. *Neural Comp and App*. 34:5321-5347.

Nunez P, Srinivasan R. 2009. Electric fields of the brain. NY: Oxford University Press. 494-497.

Oldham M, Horn P, Tsevat J, Standridge S. 2015. Costs and clinical outcomes of epilepsy surgery in children with drug-resistant epilepsy. *Ped Neuro*. 53(3): 216-20.

Osorio I, Zaveri H, Frei M, Arthurs S. 2011 Epilepsy: the intersection of neurosciences, biology, mathematics, engineering, amd physics. Boca Raton: CRC Press.

Panteliadis, C. 2021. Historical overview of electroencephalography: from antiquity to the beginning of the 21st century. *eScientific Journal of Brain and Neurological Disorders*. 3(1): 1-13.

Pelletier C, Webb G, Petitjean F. 2019. Temporal convolutional neural network for the classification of satellite image time series. *arXiv*:1811.10166v2.

Pellock J, Dodson W, Bourgeois B. 2001. Pediatric epilepsy: diagnosis and therapy. New York: Demos.

Pfisterer U, Petukov V, Demharter S, Meichsner J, Thompson J, Batiuk M, Asenjo-Martinez A, Vasistha N, Thakur A, Mikkelsen J, Adorjan I, Pinborg L, Pers T, von Englehardt J, Kharchenko P, Khodosevich K. 2020. Identification if epilepsy-associated neuronal subtypes and gene expression underlying epileptogenesis. *Nat Commun* 11, 5038.

Pradhan N, Sadasivan, P, Arunodaya, G. 1996. Detection of seizure activity in eeg by an artificial neural network: a preliminary study, *Comp Biomed Res*, 29(4): 303 – 313.

Qu H, Gotman, J. 1993. Improvement in seizure detection performance by automatic adaptation to the eeg of each patient. *Electroenceph. and Clin. Neurophys*. 86: 79 - 87.

Rasavian N, Sontag D. 2016. Temporal convolutional neural networks for diagnosis from lab tests. *arXiv*:1511.07938v4.

Robinson A, Venkatesh P, Boring M, Tarr M, Grover P, Behrmann M. 2017. Very high density eeg elucidates spatiotemporal aspects of visual processing. Scientific Reports 7:16248.

Rodríguez Quintana JH, Bueno SJ, Zuleta-Motta JL, Ramos MF, Vélez-van-Meerbeke A; , the Neuroscience Research Group (NeuRos). Utility of Routine EEG in Emergency Department and Inpatient Service. *Neurol Clin Pract*. 2021 Oct;11(5):e677-e681

Roheda S, Krim H, Jiang B. 2000. Volterra neural networks (vnns). *J. Machine Learn* I (2022): 1-48.

Rosenow F, Luders H. 2001. Presurgical evaluation of epilepsy. *Brain* 124: 1683-1700.

Ross M, Smith Michael, Alvarez M. 2021. Learning nonparametric volterra kernels with gaussian processes. arXiv:2106.05582 [stat.ML]

Russell S, Norvig P. 2020 Artificial intelligence: a modern approach. Pearson Series in Artificial Intelligence, 4th Edition.

Scharfman, H. 2007. The neurobiology of epilepsy. *Curr Neurol Neurosci Rep*. 7(4): 348-354.

Schetzen M. 2006. The volterra and wiener theories of nonlinear systems. Cornell University Press.

Schmidt, D. 2009. Drug treatment of epilepsy: options and limitations. *Epilepsy & Behav* 15: 56-65.

Seidenberg M, Pulsipher DT, Hermann B. Association of epilepsy and comorbid conditions. *Future Neurol*. 2009 Sep 1;4(5):663-668.

Shatz CJ. 1992. The developing brain. Sci. Am. 267, 60–67. (10.1038/scientificamerican0992-60).

Simonyan K, Vedaldi A, Zisserman A. 2014. Deep inside convolutional neural networks: visualizing image classification models and saliency maps. *arXiv*:1312.6034v2.

Slutzky M, Jordan L, Krieg T, Chen M, Mogul D, Miller L. 2010. Optimal spacing of surface electrode arrays for brain machine interface applications. *J Neural Eng.* 7(2): 1-20.

Smith J. 2020. A temporal neural network architecture for online learning. *arXiv*:2011.13844v2

Smith, S. 2012. Eeg in the diagnosis, classification, and management of patients with epilepsy. *J Neurol Neurosurg Psychiatry*; 76(Suppl II):ii2–ii7.

Srinivasan R, Nunez P, Silberstein R. 1998. Spatial filtering and neocortical dynamics: estimates of eeg coherence. *IEEE Trans Biomed Eng* 45:7: 814-826.

Srinivasan R, Tucker D, Murias M. 1998. Estimating the spatial nyquist of the human eeg. *Behav Res Methods Instruments Comput*. 30: 814-826.

Sufiani F, Ang L. 2012. Neuropathology of temporal lobe epilepsy. *Epilepsy Res Treat* 2012: 624519.

Szegedy C, Liu W, Jia Y. 2014. Going deeper with convolutions. *arXiv*:1409.4842v1.

Taylor P, Sinha N, Wang Y, Vos S, Tisi J, Miserocchi A, McEvoy A, Winston G, Duncan J. 2018. The impact of epilepsy surgery on the structural connectome and its relation to outcome. *Neuroimage: Clinical* 18:202-2014.

Thukral A, Ershad F, Rao Zhonlyu. 2018. Soft neural interfaces for ultrathin electrodes. *IEEE Nanotech Magazine*, March 2018: 21-34.

Toth R, Barth A, Domonkos A, Varga V, Somogyvari Z, 2011. Do not waste your electrodes – principles of optimal electrode geometry for spike sorting. *J. Neural Eng* 18: 1-22.

Valeta T, de Boer H, 2010, Stigma and discrimination in epilepsy. in: Panayiotopoulos, C.P. (eds) Atlas of Epilepsies. Springer, London. https://doi.org/10.1007/978-1-84882-128-6_201

Webber W, Lesser R, Richardson R, Wilson K. 1996. An approach to seizure detection using an artificial neural network (ann)," *Electroenceph. and Clin Neuro*, 98:250-272.

Wen CK, Hudak PL, Hwang SW. Homeless people's perceptions of welcomeness and unwelcomeness in healthcare encounters. *J Gen Intern Med*. 2007 Jul;22(7):1011-7.

Weng W, Khorasani K. An adaptive structure neural network with applications to eeg automatic seizure detection. *Neural Networks* 9(7): 1223-1240.

Wenzel M, Huberfield G, Grayden D, de Curtis M, Trevelyan. 2023. A debate on the origin of focal seizures. *Epilepsia* Dec:64 Suppl 3:S37-S48.

West S, Nevitt SJ, Cotton J, Gandhi S, Weston J, Sudan A, Ramirez R, Newton R. Surgery for epilepsy. *Cochrane Database Syst Rev*. 2019 Jun 25;6(6): CD010541.

Westwick D, Lutchen K, Suki B. 1998. Sensitivity analysis of kernel estimates: implications in nonlinear physiological system identification. *Ann Biomed Engr* 26: 488-501.

Yan J, Mu L, Wang L. 2020. Temporal convolutional networks for the advance prediction of enso. *Sci Reports* 10:8055.

Yoganathan K, Malek N, Torzillo E, Paranathala M, Greene J. 2023. Neurological update: structural and functional imaging in epilepsy surgery. *Neurological Update* 270: 2798-2808.

Zack MM, Kobau R. National and state estimates of the numbers of adults and children with active epilepsy — United States, 2015. *MMWR*. 2017; 66:821–825.

Zador A, Escola S, Richards E, Olveczky B, Bengio Y, Boshen K, Botvnick M, Chklovskii D, Churchland A, Clopath C, DiCarlo J, Ganguli S, Hawkins J, Kording K, Koulakov A, LeCun Y, Toward Next-Generation Artificial Intelligence: Catalyzing the NeuroAI Revolution. arXiv:2210.08340 [cs.AI].

Zhou S, Shen W, Zeng D. 2016. Spatial-temporal convolutional neural networks for anomaly detection and localization in crowded scenes. *Sig Proc: Image Com* 47: 358-368.